UNIVERSITY OF WATERLOO

FACULTY OF ENGINEERING

DEPARTMENT OF MECHANICAL AND MECHATRONICS ENGINEERING

MTE 481 - Final Design Proposal
TableUV - Fully Autonomous UV Disinfectious Robot

Proudly Prepared by:

Group 55

Jianxiang (Jack) Xu
Tsugumi Murata
Jerome Villapando
Dong Jae (Alex) Park

Dec. 10, 2020

Dec. 10, 2020

Prof. Ayman El-Hag
Prof. Baris Fidan
Prof. James Tung
Prof. Andrew Kennings

Department of Mechanical and Mechatronics Engineering
University of Waterloo
Waterloo, Ontario, Canada

Dear MTE 481 Course Instructors,

This report, entitled 'TableUV - Fully Autonomous UV Disinfectious Robot' was prepared as the MTE481 FYDP Final Design Proposal Report. It entails a design process and proposal for our final FYDP idea on a palm-size autonomous UV disinfectious robot. This report will go over engineering design processes from Mechanical, Electrical, and Software perspectives.

In preparation for 4A, early stage brainstorming meetings were already conducted throughout the summer term of 2020 to get an understanding of what type of problems needed to be solved, and to determine technologies that can be used to solve the problem. Mechanical and electrical prototyping of different sensors and actuators were performed to explore the performance and feasibility of its implementation. This early prototyping rewarded the group early on, as the initial idea of vacuum robot was determined to be unfeasible due to its challenges on the vacuum mechanism.

During the 4A term, MTE 481 helped the group narrow down the exact problem to solve and understand the constraints and criteria that needed to be set in place to guide the project forward. As shown throughout the report, numerous advancements in mechanical, electrical, and software design were made during the term. With this, the team is placed in a great position to develop, test, and debug in time before the end of the fall term.

We would like to appreciate the help from the MTE 481 instructors, and Professor Marc Aucoin from Chemical Engineering whom have actively provided supportive feedback and resources throughout this intense 4A study term.

This report was written entirely by us and has not received any previous academic credit at this or any other institution.

Sincerely,
Jianxiang (Jack) Xu, Tsugumi Murata, Jerome Villapando, Dong Jae (Alex) Park

Jianxiang Xu Tsugumi Murata Jerome Villapando Dong Jae Park

Table of Contents

List of Figures

List of Tables

Summary

A study has been conducted to show a need to reduce surface transmission of diseases. The current solution is to disinfect with tools manually, but there is lack of fine control and certainty in this method. Autonomous solutions have been emerging but are very expensive and bulky. The goal of this project is to fill that gap in the market and create an autonomous solution that is cost-effective and relatively small which can be used to disinfect surfaces in public spaces in order to reduce disease transmission.

Constraints and criteria are put in place to guide the direction of this project. There are constraints placed on amount of disinfection, ability to avoid obstacles, ability to stay on the surface, supported weight, cost, safety, and disinfection effectiveness. The main criteria to consider are size, surface coverage, environment adaptability, production cost, and cleaning time.

In early design studies, four designs were considered to meet the goals of this project. The mobile manipulator, swivel arm, drone, and tabletop standalone robot had their positives and negatives weighed in terms of ability to meet the chosen constraints and criteria. In the end, the tabletop standalone robot is chosen for many factors such as simplicity, efficiency, and low cost. Furthermore, the design will have six key components: a drive train system, sanitization system, sensing system, computing and communication system, power system, and a chassis. In deeper detail, the mechanical, electrical, and software design is developed accordingly.

The mechanical design involved designing a chassis CAD model to house all the necessary components that make up the robot. The main challenge is the ideal placement of sensors in order to acquire the most useful information about the environment as possible. Placement of key disinfection systems is also important in order to maximize performance of disinfection to the fullest.

The electrical design involved choosing the components and designing an electrical architecture to connect the components with their systems accordingly. For example, a power budget estimate was conducted to get an idea of the system's power requirements which was used to select the main battery for the power system. With the main components selected, the system architecture is developed with four main subsystems: the MCU board, power board, sensor board, and the driver board. In addition, work is done on modelling, simulation, and electrical CAD to prepare for manufacturing.

The software design involved thinking about the planned motion of the robot with simulation. Great consideration was made on the whole process the robot will take as a system. The designed system process includes the algorithm to perform localization/mapping, and the algorithm to perform surface disinfection. For visualization, simulations were performed using Webots and MATLAB. Additionally, the motion model of the robot is calculated based on the kinematics of the design which will be useful later for localization.

Moving on, verification is performed to ensure that some of the designs in place are meeting the chosen constraints and criteria. To verify the selected motor's performance, calculations were made based on the theoretical load on the robot. An additional physical test on a prototype drive train is also conducted for further verification. To verify sensor placement, the sensor's effective sight radius is modelled in CAD. To verify the constraint on robot life, battery capacity calculations were referenced. To ensure handling of motion and safety edge cases, sensors and hardware features were selected and designed to prevent unfavourable situations. To verify performance of robot motion and obstacle avoidance, research on path planning and sensor section were referenced.

Lastly, a timeline and budget was made as of the end of the Fall term, with some key expectations rolling into the Winter term.

1 Introduction

2020 has been a pivotal year in modern history, and not just because of all the negative events, but because this year has brought to light a problem that has been occurring pre-COVID-19. Last year in the US, more than 2.8 million people were afflicted with an antibiotic-resistant infection, not including viruses such as HIV and influenza [1]. Unfortunately, as a result, these infections lead to the deaths of 35,000. In our Capstone group, we have a vision to significantly reduce disease transmission by designing an accessible and economical device for the general public.

1.1 Background

Due to the recent global pandemic, disease transmission become a major concern in terms of disease control. Although masks and a frequent hand-wash habit can effectively reduce the risk of infection, public tables can be a secondary source for disease transmission since the bacteria and virus can remain on surface alive for more than 2 hours and even days depending on the surface condition and environment condition [2].

1.2 Needs Assessment

Again, masks and a frequent hand-wash habit can effectively reduce the risk of infection, but common surfaces can be a major source of disease transmission as well. Because of this, we want to target reducing transmissions through surfaces, specifically targeting objects in public areas that are meant to be shared with numerous people. This device will be targeted towards institutions with common areas shared by the general public which have high risk in accelerating transmission of diseases. Some examples include restaurant tables, community library tables, classrooms, reception desks, and hospitals. The current solution of disinfection is by manual labor which somewhat defeats the purpose of the action because it not only puts the cleaner at risk, but it also makes the cleaner as a source of transmission. In addition, the effectiveness of the person's method of disinfection is not controlled nor measured meaning that cleaning effectiveness is not guaranteed. Moreover, some autonomous solutions cost over $100,000 which are often bought solely by medical institutions that have rich budget to stomach that cost [3]. Even if the current autonomous solution were to lower its price, its bulkiness is not suitable for tabletops, and will require people to evacuate the room to start disinfecting for safety reasons. This Capstone device aims to fill the gap in that market by designing an autonomous and affordable solution to disinfect surfaces.

1.3 Problem Formulation

Conventional disinfection robots are expensive and require people to evacuate before use for safety concerns. There is a need to design and implement an affordable and autonomous mechatronic system capable of successfully disinfecting surfaces in public spaces to reduce disease transmission.

1.4 Constraints and Criteria

1.4.1 Constraints

I The robot must be able to disinfect at least one table of $1.2\,[\mathrm{m}] \times 0.7\,[\mathrm{m}]$ in one charge.
II The robot must be able to operate safely on the table top without knocking off objects.
III The robot must be able to stay on the tabletop without exceeding its boundary.
IV The robot must be able to support a minimum load of $1\,[\mathrm{kg}]$ including the robot weight.
V The cost of production must be cheap enough to be considered as a viable product for restaurants, libraries and other public spaces $<$ \$300CAD.
VI The robot must pose minimum risk to nearby people (such as UV exposure).
VII The robot must be able to sanitize $> 99\%$ of common bacteria and viruses including SARS-CoV-2.

1.4.2 Criteria

I The robot must be small enough such that it does not occupy the tabletop space. (Ideally a palm-size within $1000\,[\mathrm{cm}^3]$).
II The robot must be able to cover a wide surface area of the table.
III The robot must be adaptable for it to be used in various environments.
IV The production cost of the robot must be minimized.
V The robot must clean a standard table ($1.2\,[\mathrm{m}] \times 0.7\,[\mathrm{m}]$) within $30\,[\mathrm{min}]$.

2 Proposed Solutions

2.1 Preliminary Solutions

During the design selection phase, the team came up with 4 preliminary concept solutions that were critically analyzed for selecting the final design. This section provides a high-level overview of the preliminary designs generated.

2.1.1 The Mobile Manipulator

The mobile manipulator mainly consists of a robotic manipulator arm mounted on top of a mobile platform. Ideally, the mobile platform would be able to localize and map its environment to be able to maneuver around its environment to disinfect multiple tabletops. The end effector of the manipulator could house a disinfection mechanism consisting of a disinfectant spray and a UV light emitter. This solution eliminates the need for multiple robots as a single robot cab handle and manage multiple tabletops. Additionally, with such a versatile system, the robot could be designed to be multi-purposed; organizing dishes and cutlery as well as serving dishes to tables.

However, this design was deemed unfeasible in terms of project scope and time for the FYDP. Additionally, purchasing or building a mobile manipulator full with a base and an arm would be expensive and thus is not affordable for the targeted users.

2.1.2 The Swivel Arm

The ”Swivel Arm” was a second iteration of the mobile manipulator as it bore many similarities with the first design. Like the mobile manipulator, it would be capable of maneuvering around its environment, but the robotic arm would be replaced with a simpler swiveling arm that has a single degree of freedom. This vastly reduces the complexity of the system while maintaining the capability to disinfect the tabletop surfaces. To better illustrate the concept, a preliminary sketch of the concept is provided below.

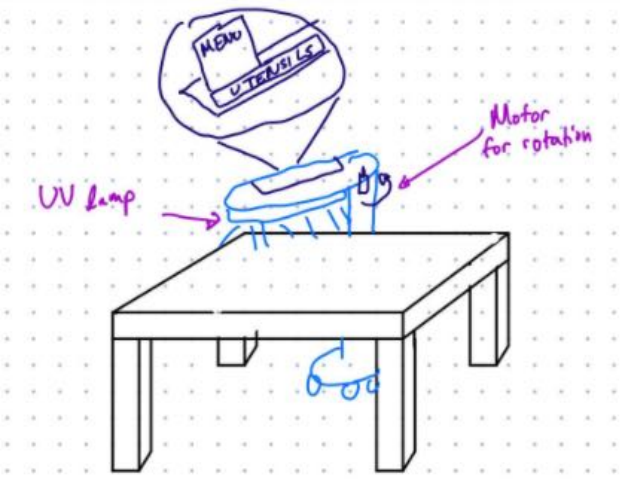

Figure 2-1. Sketch of Swivel Arm Design.

2.1.3 The Drone

This design consists of a drone equipped with a disinfectant mechanism to allow 3D operation. This allows for an easy traversal between different tables, and also allows for the robot to disinfect surfaces such as chairs and arm-rests. However, due to the high level of noise pollution and its high risk of indoor operation, the design was elimiated.

Figure 2-2. An image of NUI's UVCDrone in action. [4]

2.1.4 The Tabletop Standalone version

This idea focused on making the design compact so that the robot can operate and live on the tabletop itself. Limiting the operation environment to the tabletop only will reduce the component size and cost, thereby making the unit solution affordable. The downside for this design is that for an efficient operation, a robot per table will be needed.

2.2 Selected Proposed Solution

Based on the constraints and criteria listed in Section 1.4, the tabletop standalone solution is selected due to its simplicity, efficiency, and low cost. Hence, the proposed conceptual solution is shown as the sketch in Figure 2-3, with a similar system as a generic Roomba robot. In general, the robot will consist of six core components: a drive train system, sanitization system, sensing system, computing and communication system, power system, and a chassis.

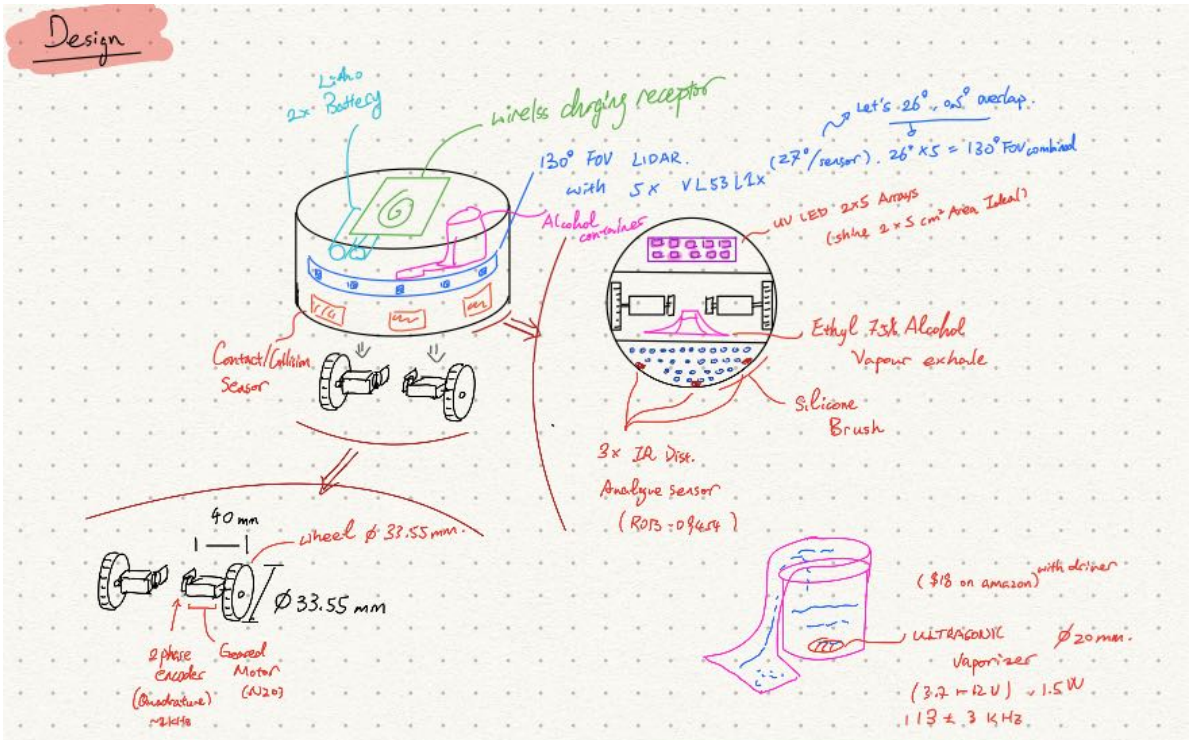

Figure 2-3. Sketch of the proposed solution (Mechanical)

First of all for the drive train system, a two wheel differential drive system is used for the table-top maneuvering. Since a two wheel drive system allows linear or curvature motions, it is ideal for cleaning a standard square and round table. In addition, two wheel drive system is easy to create a motion model for simu-

lation, therefore simplifying the motion complexity and pose estimation for later software developments. Moreover, two wheel drive also simplifies the mechanical design.

In terms of sanitization system, a combination of UV LEDs and alcohol spraying system is used to effectively and efficiently disinfect viruses such as COVID, bacteria, and germs. With simple calculation on power estimation and timing budgets, it is found an array of 2×5 UV LEDs for a coverage of $10\,[\text{cm}^2]$ area would only require $8.5\,[\text{min}]$ to clean a standard 4-person table ($122 \times 76\,[\text{cm}^2]$) for an $\eta = 99\%$ effectiveness (as recommended in Constraint VII) with an exposure energy of $3.5\,[\text{mJ/cm}^2]$. In addition, the alcohol spraying system is inspired by the modern vaporizer in the humidifier, which uses ultrasonic actuator to vaporize the liquid in form of water droplet. The idea is to use such ultrasonic actuator to vaporize the 70% alcohol to the tabletop surface to ensure an even coverage of small Isopropyl alcohol droplet at the prior or the end of the UV exposure. This will permit an additional sanitization layer to kill general bacteria and germs.

The sensing system combines two sets of systems: a set of localization feedback system and a set of environment perception system. For localization, a combination of 2-phase motor encoders and a 9-Axis IMU sensor is used to estimate the robot pose. For environment mapping, a set of three ToF sensors are used to perform surrounding mapping and active SLAM along with the internal localization system. In addition, a set of three IR analog distance sensors are used for table edge detection. Lastly, there are frontal collision sensors for emergency stop in case of unprecedented obstacles in the field.

In terms of computing and communication system, an ESP32 chip is used as the main computing host. Since ESP32 has a dual core with $240\,[\text{MHz}]$ clock speed, it is fair enough to handle most light weight SLAM tasks and low-level controls. In addition, it is fairly cheap with a cost around \$3 $\sim$ 5 CAD (as preferred by Constraint V and Criterion IV) and is widely used in the open-source community with wide range of supports available. It has all the communication protocols needed to interface with all sensors as shown in Figure 2-4 below. Lastly, it is capable of wireless communication via Bluetooth and Wifi, so it can handle OTA update and synchronization later if decided to be adopted. The wireless system can also be used to display and alert status of the robot to user's smartphone.

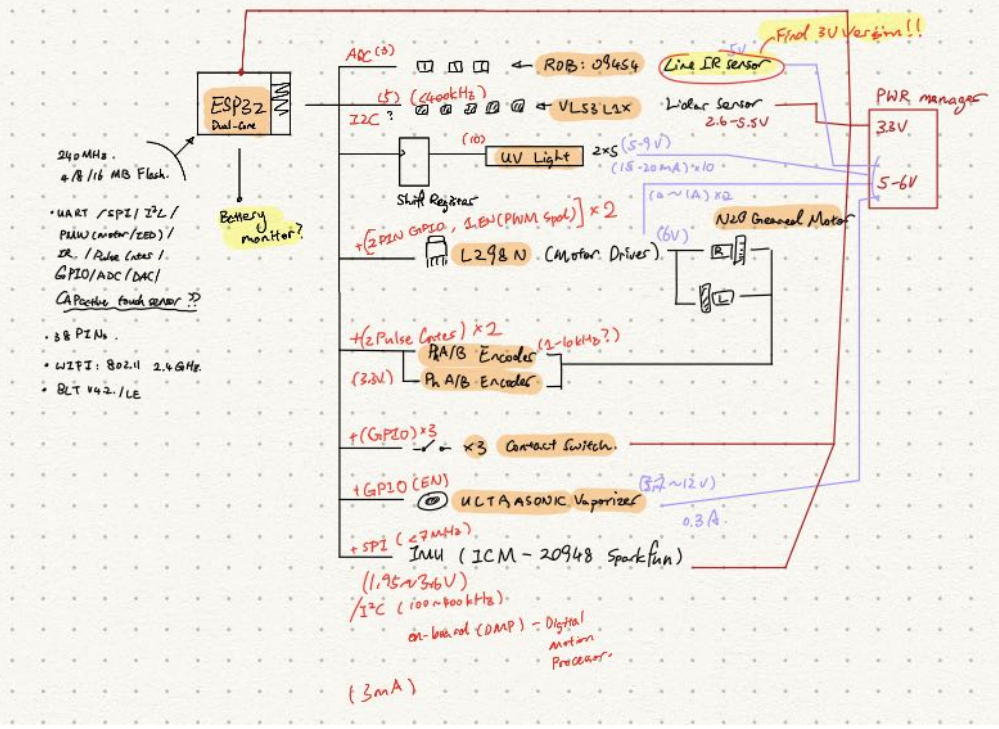

Figure 2-4. Sketch of the proposed solution (Electrical)

The power system handles the power distribution and charging conditions. As shown in Figure 2-4, there are many sensors and actuators that are operating in different voltage ranges and with different power requirements, hence, a dedicated distribution should be designed to convert and stabilize the voltage from the battery.

Finally, for a chassis design, the robot would be in a form of simple cylindrical shape. With a cylindrical body, the robot would not need extra sensing capabilities when performing rotation with a two wheel drive system. Hence, there is only need to design sensing system for the frontal collision only, to reduce the component cost and complexity of the robot. And the main prototype manufacturing process is 3D printing for its low-cost and low-complexity process during the prototype phase.

3 Detailed Design

In this section, the detailed design of the proposed solution (Section 3.1) and its analysis (Section 3.2) would be discussed from Mechanical, Electrical, and Software aspects.

3.1 Design of the Proposed Solution

3.1.1 Mechanical

As described in the proposed solution in Section 2.2, the mechanical aspect should cooperate with the sensor placements and sanitization factors. With the conceptual sketch in Figure 2-3, the robot is designed in CAD with some calculations performed to ensure the constraints and criteria are satisfied as later discussed in Section 3.2.1 and Figure Appendix A-3. As the labelled exploded view of the robot shows in Figure 3-1, the majority of the components are retained from the proposed conceptual sketch in Figure 2-3, with some additional modifications to accommodate the software needs.

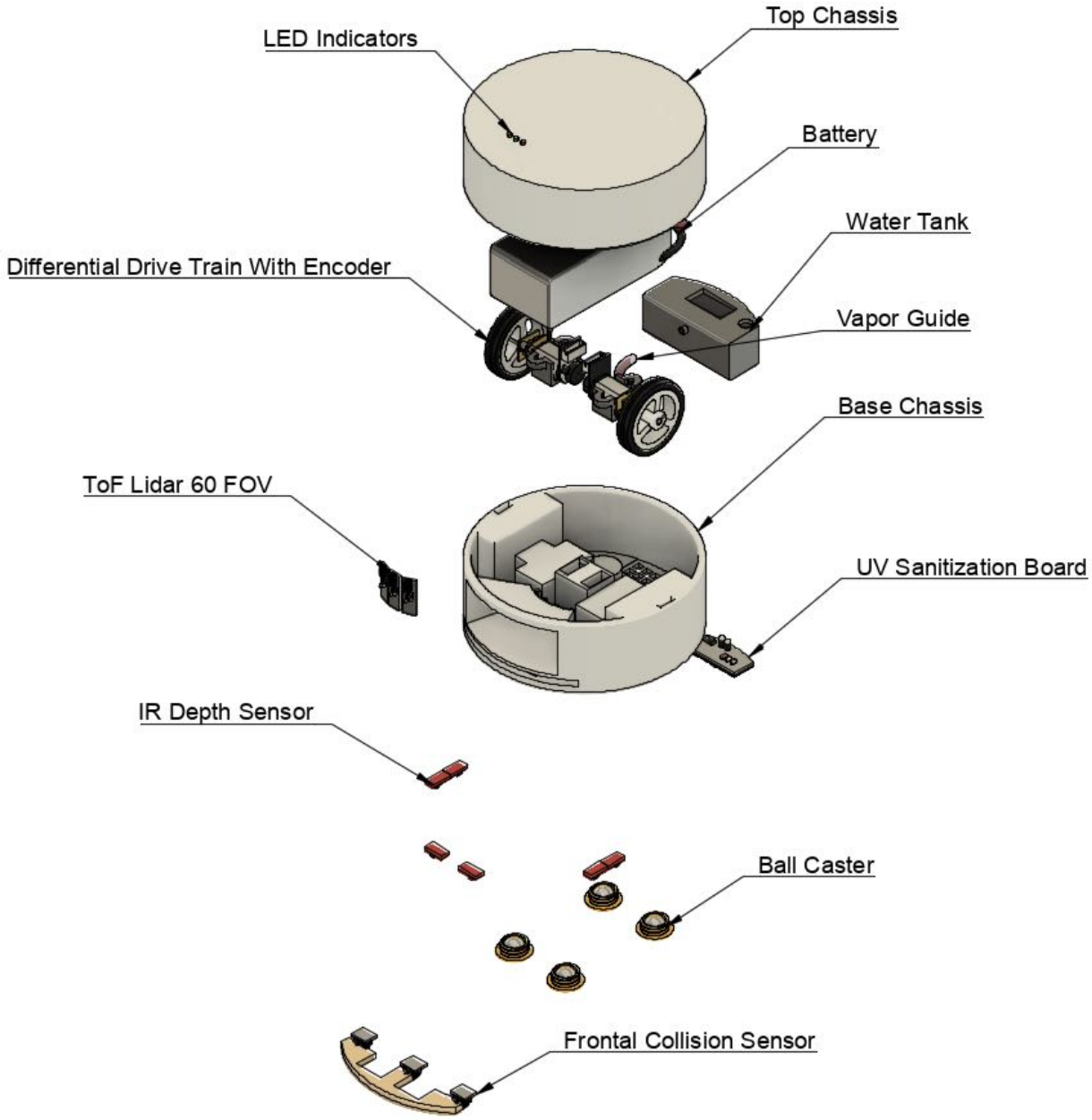

Figure 3-1. Detailed mechanical design in CAD (Exploded View) with labels

More specifically, for sensor components, there are additional IR sensors placed at the bottom of the base layer of the robot (as shown in Figure 3-2). In total, there are 3 sets of two paired IR sensors in front, left, and right side of the robot. As later mentioned in detailed Software design in Section 3.1.3, two sets of side IR will be mainly used to assist edge mapping in the initial state of the cleaning to generate an enclosed arena for better localization and path planning. This also increases the robustness to prevent the robot falling off from the table (Constraint III).

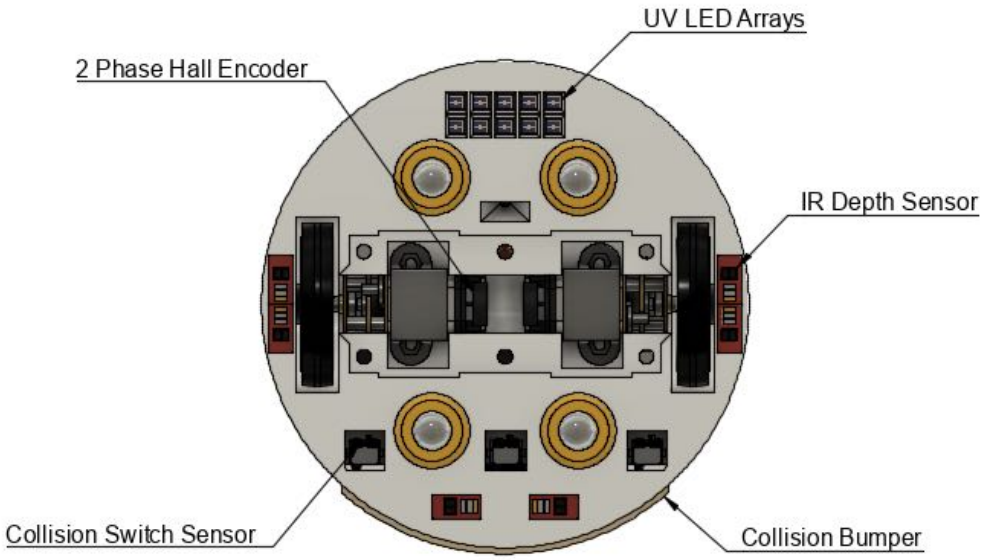

Figure 3-2. Detailed mechanical design in CAD (Bottom View) with labels

As shown in Figure 3-2, there are three collision switches as redundancy in safety in advance of any unprecedented switch failures. Moreover, with three sensors, it is also possible to estimate the impact energy and attacking angles based on the vehicle motions and the difference in timing budgets among the switches upon impact. To note, switches here are implemented in case of unexpected intruders and obstacles that were not picked up by the ToF sensors, since the sensors has a small gap ($\approx 10\,[\text{mm}]$) of blind zones highlighted as red triangles in Figure 3-3 and Figure Appendix A-7.

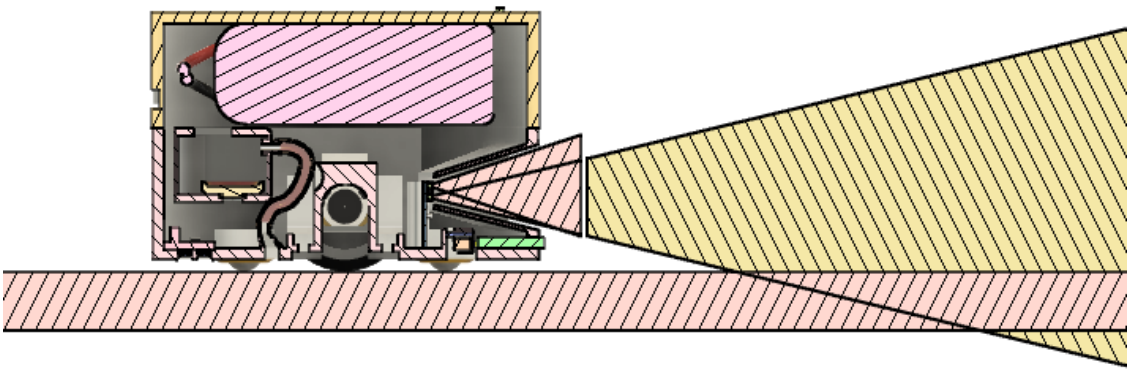

Figure 3-3. Detailed mechanical design in CAD (Cross-section View)

In addition, the steam exhale is now placed in the rear section of the robot between the UV arrays and the drive train, as shown in Figure 3-3. There would be a tube guide connecting from the ceiling of the chassis to the water tank for refilling rubbing alcohol (not shown in this design). Moreover, the battery would be hanging over the ceiling in chassis along with the computing board and power distribution board,

also shown in Figure 3-4. To note, the two metal contact blocks sitting in the slot at the rear side of the top chassis are the main magnetic charging port. There is a projected future design for a self docking station to increase the process of the automation, and a water-proof version to allow easy cleaning and even self cleaning with the docking station.

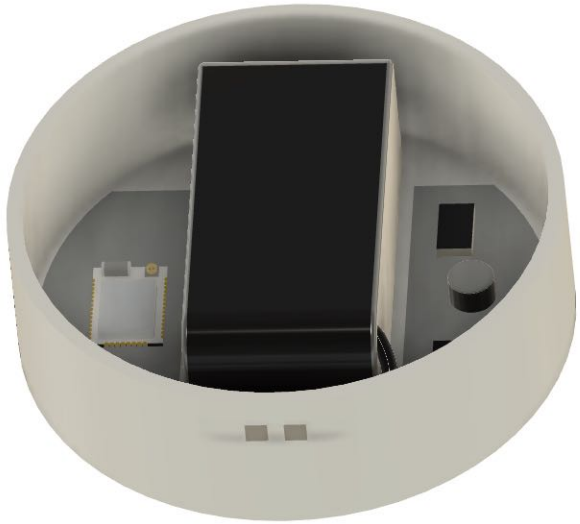

Figure 3-4. Detailed mechanical design in CAD for computer and power placements in top section

3.1.2 Electrical

3.1.2.1 Component Selection

Component selection is done by reviewing the required specification of the robot, and then selecting corresponding actuators and sensors. For example, the ToF sensor, VL53L1X [5], is selected from various sensors due to its low cost, configurable ROI, small dimension, long range, and low current consumption. The full list of components selected in shown in Figure Appendix D-2.

3.1.2.2 Power Budget

With component selection completed, the power budget of the system is calculated for the electrical system. This is done by separating each loads by respective power rail, and then calculating the nominal and max current consumption with 10% margin. This calculation is then used to analyze the robot operation time and to select suitable battery. The full calculation is available at Figure Appendix C-2 and summary of each rail is shown below in Table 3-1.

Table 3-1. Summary of power budget for each rail

Rail Voltage (V)	Nominal Current (A)	Max Current (A)
3.3	1.21	1.34
6	1.0	2.0
10	0.22	1.65
24	0.25	0.25
TOTAL	2.68	5.24

3.1.2.3 Power Architecture and Battery Selection

With power budget information available, the power architecture design and battery selection is conducted. Since the source will be a rechargeable battery, the source rail will be in multiplier of 1.5V if Ni-MH is used, and 3.7V if Li-Po/Li-ion is used [6]. The list of candidate batteries is shown at Figure Appendix C-3. Battery with lower source voltage will have smaller battery dimension and lower cost, but since the required rails are relatively high, the current consumption from the battery side will be much higher.

Therefore for battery selection, calculation table is created as shown in Figure Appendix C-4. This table calculates the current consumption at the battery's source voltage level, and checks if the robot's battery consumption in mAh is under the battery's capacity, and whether the battery's discharge rate is sufficient for the robot's consumption or not.

Based on the calculation table and consideration with cost and size, GOLDBAT 1500mAh 11.1V 100C 3S Lipo[7] is selected as the battery.This battery is 3 cell battery, meaning 11.1V, and has 1500mAh capacity with 100C discharge capacity.

The calculation summary for this battery is shown below in Table 3-2. Notice that the selected battery satisfies the required specs.

Table 3-2. Calculated parameter of selected battery

Calculation Parameter	Calculated Value
Total Battery Current Consumption (mA)	4010.42
Operation Time (h)	0.167
Operation Battery Consumption (mAh)	668.40
Required Discharge Capacity (C)	2.67

3.1.2.4 System Design

Figure 3-5 shows the designed electrical system diagram for the robot. This robot will be comprised of four electrical subsystems: the MCU board, power board, sensor board, and the driver board, and the respective PCB necessary is indicated with the green box in the diagram. The boards are broken by subsystems to meet the small dimension of the robot, and custom designed circuits are used instead of off-the-shelf components as much as possible to reduce the cost.

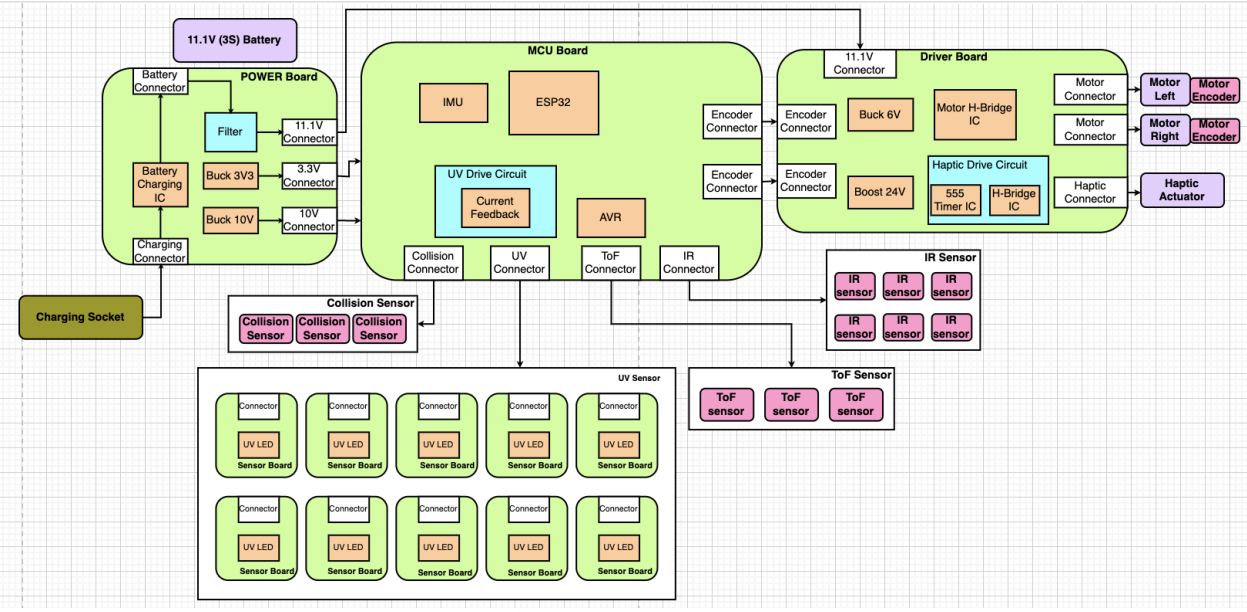

Figure 3-5. Electrical System Diagram

The MCU board is the central board that communicates with the other boards to send control signal, and to receive and process sensor data. It contains the ESP32 [8], on board IMU sensor, necessary sub-circuit for UV and ToF sensors, and various connectors to interface with the other boards.

The power board interfaces and distributes the power to the other boards in the robot. It will receive the 11.1V battery which is initially filtered and then converted to the required rail level using DC-DC converters. 3.3V and 10V is created using buck converter which is then distributed to the MCU board. 10V is used for powering the UV LEDs, and 3.3V is used to power the other components such as ESP32[8] and IMU[9].The battery voltage, 11.1V, is passed to the driver board directly since the rail conversion is done on the driver board side.

The sensor board will be designed for UV LED only since low cost breakout boards will be used for ToF[5] and IR[10] sensor, and collision sensor only needs wire connection to be used.

Lastly, the driver board is responsible for driving the motors and the piezo actuator. The power rail required for motor and piezo drive, 6V and 20V respectively, are created on the driver board side to reduce cable connection between the power board.

3.1.2.5 Modelling

To verify that the designed circuit works and satisfies the requirement, simulation is conducted using LT-Spice[11]. For majority of the components, the manufacture provides a SPICE model that can be used in the simulation but for some components, these models are not available and hence needs to be made. The SPICE model for UV LED is made to allow the UV LED drive circuit to be simulated, and is shown below Figure 3-6. Notice how the designed model's I-V characteristic matches that on the datasheet.

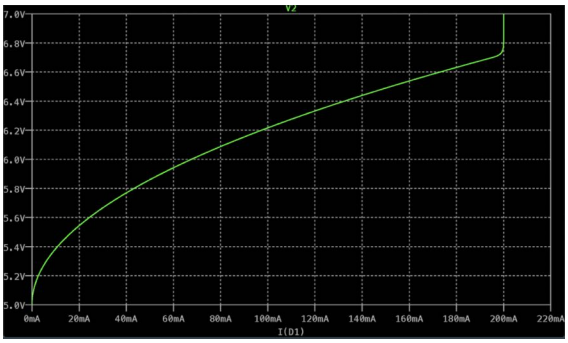

(a) Desgined LTPL-G35UV275GR-E model I-V curvel

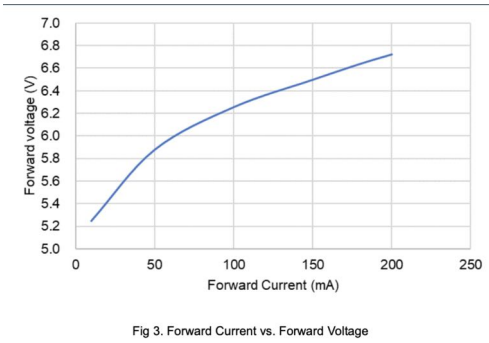

Fig 3. Forward Current vs. Forward Voltage

(b) LTPL-G35UV275GR-E datasheet I-V curve

Figure 3-6. Comparison of the I-V curve between designed model and datasheet

3.1.2.6 Simulation

With the UV LED model created, the designed UV LED drive circuit is simulated. The purpose of this circuit is to allow the MCU to control the power intensity of the LED, and thereby the disinfection ability. This is done by control current circuit, and since the ESP32 features a DAC, this is used to provide the reference voltage to the control circuit. Additionally, the drive circuit features a hardware shutdown circuit which is enabled when the IR sensor exceeds the threshold voltage. This forces the UV to power off when the robot is not on the table to prevent unnecessary UV exposure to the user. The simulated circuit and simulation result is shown in Figure 3-7.

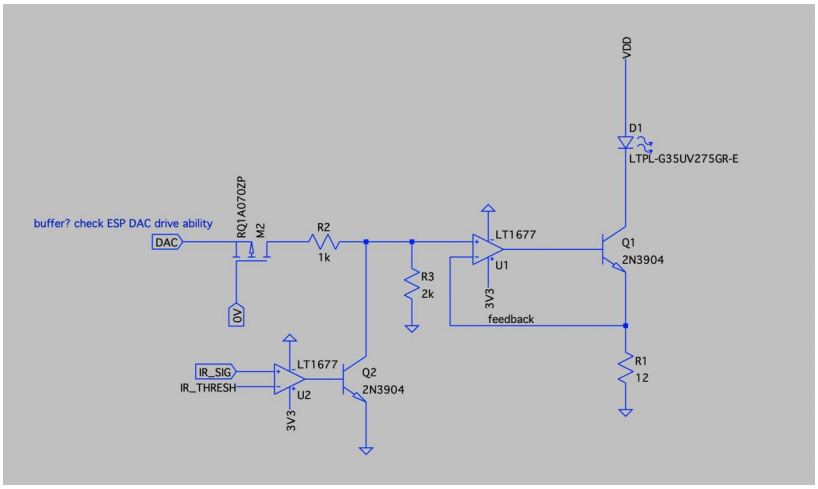

(a) UV Drive Circuit Design

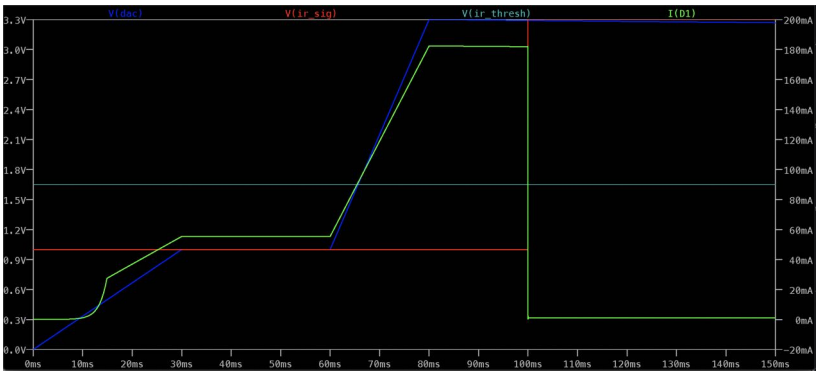

(b) UV Drive Circuit Simulation Output

Figure 3-7. Circuit and Simulation of UV Drive Circuit

Similarly, the simulation for piezo drive circuit is conducted and shown below in Figure 3-8. The piezo drive circuit creates an AC signal output at the required resonant frequency of the piezo actuator. For piezo drive, proof-of-concept was conducted by purchasing off-the-shelf piezo drive circuit [12] (setup in Figure Appendix B-1).

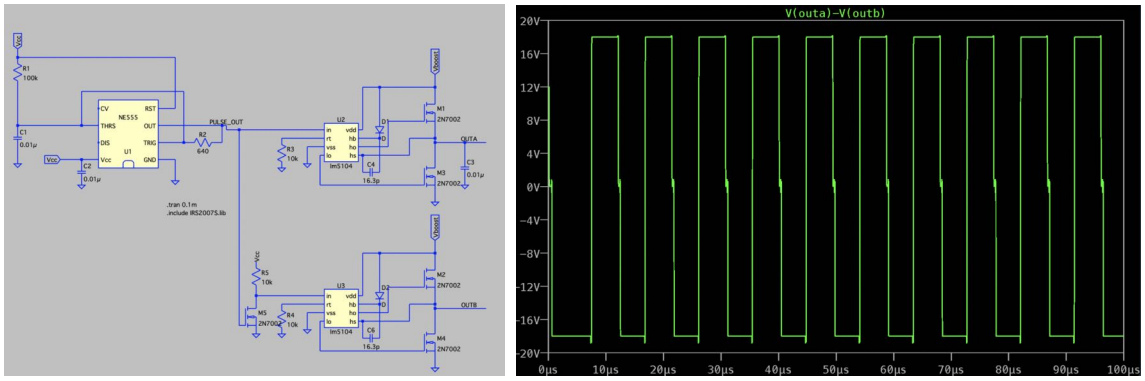

(a) Piezo Drive Circuit Design (b) Piezo Drive Circuit Simulation Output

Figure 3-8. Circuit and Simulation of Piezo Drive Circuit

3.1.2.7 Schematic and layout

After the designed circuit is simulated, the design is implemented in CAD to be made as a PCB. The schematic and layout design is in progress as of now, and therefore the fully completed PCB of UV Sensor Board is shown below in Figure 3-9.

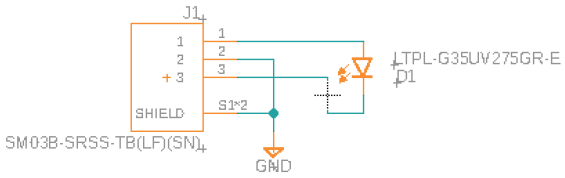

(a) UV Sensor Board Schematic

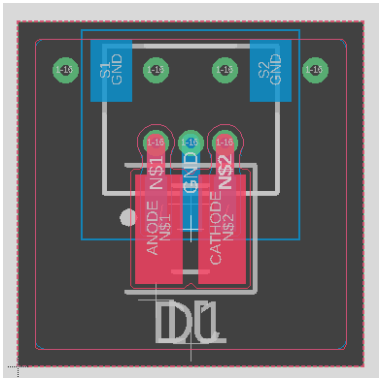

(b) UV Sensor Board Layout

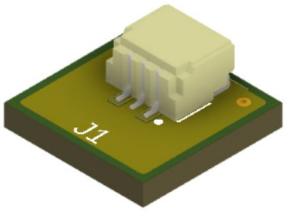

(c) UV Sensor Board 3D Board

Figure 3-9. UV Sensor Board Schematic and Layout

3.1.3 Software

The software design addresses problems such as acquiring data from the sensors e.g. ToF Lidar, Encoders, IR Depth Sensors, Frontal Collision Sensors and processing them to determine the state of the robot and its environment.

One of the most important task to be handled is localization and mapping. It is important for the robot to have a good belief of the map along with the locations of various obstacles as well as its own position and orientation. Therefore, in the initial phase of the robot, it tries to find the edge of a table using the IR Depth Sensors. Once an edge is determined, it then performs an edge following algorithm which moves the robot along the edge until it reaches the initial position. Using the IMU and motor encoders, we can begin mapping the environment using the ToF sensors. After the mapping is complete, the location of the homing station will be known by the robot along with its position in the table.

Using the generated map, we perform the path-planning phase, which aims at finding a collision-free path from the starting to the end point. However, for a disinfection robot this path must not simply be the shortest path. It must aim at providing a complete coverage of the surface area of the table for cleaning. There are various path planning algorithms that provide complete coverage of an area which can be categorized into either a random coverage or a pattern coverage.

Random coverage is where the robot follows a straight line in a random direction until it hits an obstacle. Once hit, a new random orientation is determined and moves along that path until another obstacle is met, forming a loop. This method is simple to implement and provides complete coverage of an area but could lead to redundant paths and more time to complete. Additionally, there are edge cases called the ”Corner Escape Angle” in which the robot can get stuck at corners. Thus, this algorithm would be suitable for domestic robots that have no time restrictions.

On the other hand, a pattern coverage method involves defining a pattern like path over the map of interest that provides complete coverage. This method has several advantages over the random coverage method as it is relatively faster compared to random coverage and does not have redundant paths.

3.1.3.1 Spiral Motion

For this motion, the robot follows an increasing/decreasing circle. This motion can be achieved by setting one of the wheels to be at full speed while increasing/decreasing the other wheel speed to generate a circular motion. The spiral can also be translated into a rectangular spiral where the robot moves in a straight line and turns 90 deg at the end of a line. Such a motion provides quick coverage of the surface area.

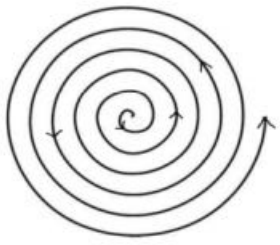

Figure 3-10. Path generated by a circular spiral algorithm.

3.1.3.2 Zig-Zag Motion

The zig-zag motion resembles the motion of a snake. This algorithm is also considered to be the fastest in terms of being able to cover the entire surface area. [13]

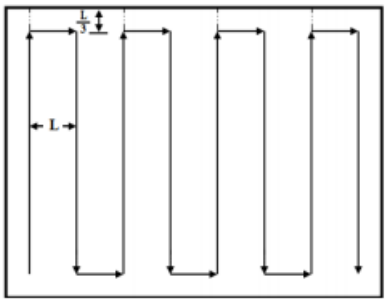

Figure 3-11. Path generated by a zig-zag motion algorithm.

During the process of the robot, if the battery indicates that charging is required, the robot would initialize the homing and charging sequence autonomously to maneuver itself to the homing station where it can be charged. Such an action would require a complete map of the environment and a good estimation of its current pose. If both are known, a motion planning algorithm such as the Bug Algorithms or Trajectory Rollout can be used to reach the goal.

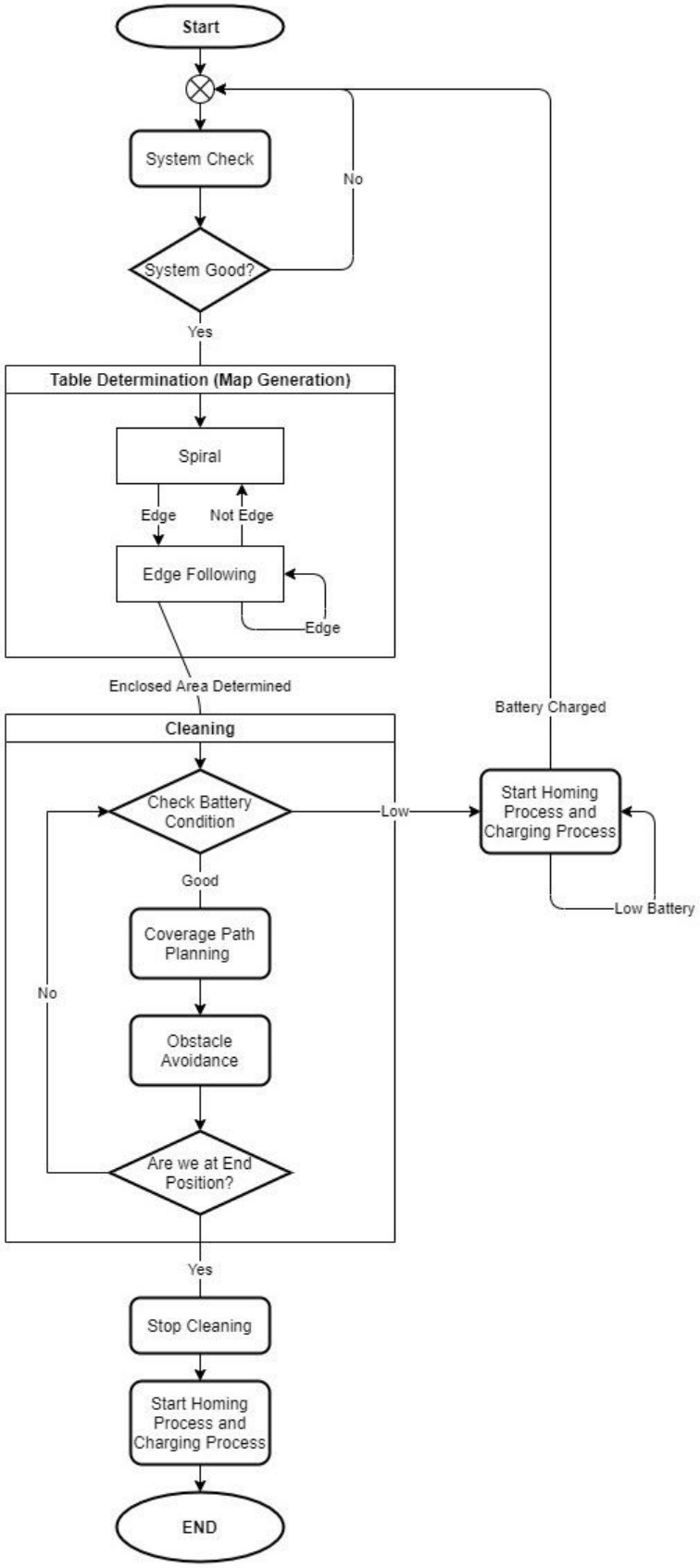

Figure 3-12. Simplified process of the robot.

3.1.3.3 Simulation

In order to provide an accurate representation of the environment in which to test the robot, an open-source 3D robot simulator, Webots, is used along with MATLAB for calculations. Having a good simulation allows us to test different algorithms and determine any flaws in out system through the visual feedback of how the robot behaves in the environment.

A CAD model of the complete robot is imported into the virtual environment which consists of a node tree that defines the environment and the robot. Several parameters such as how the different parts of the robot are connected together, their physical properties such as weight and collision meshes are all defined. The sensors and their characteristics also need to match with our real system.

In this virtual environment, the robot is placed on top of a rectangular table of $(1.2\,[\mathrm{m}] \times 0.7\,[\mathrm{m}])$ in size is placed. In addition to the robot, a series of obstacles are added to replicate a typical scenario of a table in a restaurant and also to verify the robot's obstacle avoidance operations. Additionally, Webots has MATLAB integration, allowing for the use of controllers that are designed in MATLAB to be used to control the robot.

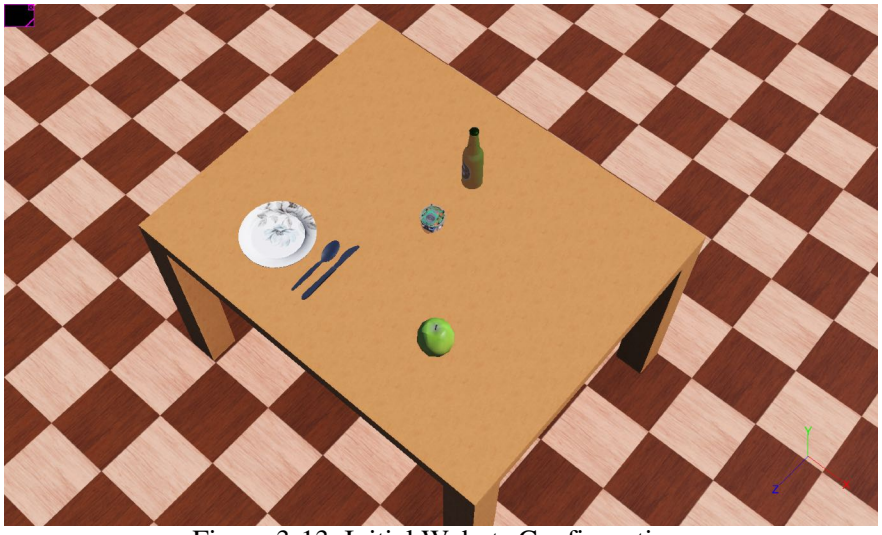

Figure 3-13. Initial Webots Configuration.

Initially, we designed a differential drive kinematic model for the robot. A differential drive robot has two main wheels each with its own motor. Additionally, caster wheels are placed which passively rolls along the floor, preventing the robot from tipping over. The dynamics of the model is not considered in this scenario as our robot will run in speeds where the forces and torques will have minimal impact.

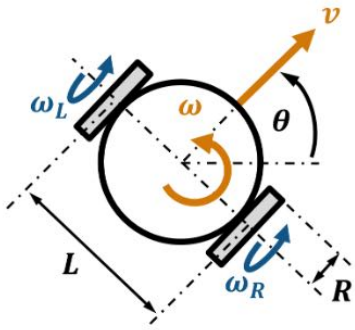

Figure 3-14. Differential Drive Model. [14]

Where:

R = Wheel Radius [m]
L = Base Length [m]
v = Linear Velocity [m/s]
ω = Angular Velocity [rad/s]
ω_R = Right wheel speed [rad/s]
ω_L = Left wheel speed [rad/s]

Therefore, to construct the mode, only the wheel radius R and the base length L needed to be set.

$$v = \frac{R}{2}(\omega_R + \omega_L) \tag{1}$$

$$w = \frac{R}{L}(\omega_R - \omega_L) \tag{2}$$

$$\begin{bmatrix} x_t \\ y_t \\ \theta_t \end{bmatrix} = \begin{bmatrix} x_{t-1} + \frac{R\omega_{R,t} + R\omega_{L,t}}{2} \cos\theta_{t-1} dt \\ y_{t-1} + \frac{R\omega_{R,t} + R\omega_{L,t}}{2} \sin\theta_{t-1} dt \\ \theta_{t-1} + \frac{R\omega_{R,t} - R\omega_{L,t}}{2L} \cos\theta_{t-1} dt \end{bmatrix} \tag{3}$$

Using the motion model defined above, a controller which takes in as inputs the wheel velocities can be used to determine the state of the robot at the next time step.

3.2 Design Review

3.2.1 Mechanical

To ensure a successful detailed design, a few calculation has to be performed to determine if the components selected for the system is within the given constraints and criteria in Section 1.4. In addition, sensor selection and placements would be discussed from the mechanical aspect point of view with considerations of the given constraints and criteria in Section 1.4.

For the drive train, a pair of micro gear motors with right amount of motor speed in RPM and torque is needed to be determined from the vendor list. With an estimated robot weight of 700 [g] and minimum constraint requirement of 1 [kg] (in Constraint IV), the wheel is required to operate with a total load of 1 [kg]. With the selected N20 micro-gear motor with 75:1 gear ratio, the motor is capable of handling a stall torque of 1.4 [kg · cm] with 410 [RPM] no-load speed [15]. As a result, the formulated load would be approximately 1.04 [kg] with each wheel and estimate tire static friction of $\mu_{static} = 0.08$ and tire diameter of $D_{wheel} = 33.5$ [mm] via the formulation in Equation (4).

$$m_{load} = \frac{N_{support}}{g} = \frac{F_{tire}}{\mu_{static} \cdot g} = \frac{\frac{\tau_{stall}}{D_{wheel}/2}}{\mu_{static} \cdot g} \tag{4}$$

As a result, the selected motor satisfies the constraint with $m_{load}^{static-single-wheel-drive} = 1.04\,[\text{kg}] \geq 1.0\,[\text{kg}]$ from the starting torque for a single wheel. Ideally, with the torque from two wheels, it is able to drive up to 2 [kg] load, hence it is capable to withstand the load requirement (Constraint IV) through most common table-top surfaces (Criterion II). Lastly, these motors are also validated with a simple setup of the two wheel drive system is tested with a load of 1.26 [kg] at 7.5 [cm/s] speed Figure 3-15.

Figure 3-15. Motor test with an additional load of 1.26 [kg]

The max speed of 7.5 [cm/s] with a load of 1.26 [kg] is fairly enough with consideration of the required top speed of 6.45 [cm/s] for 90% disinfection effectiveness (as shown in Figure 3-16). As for a 99% disinfection effectiveness (required in Constraint VII) requires twice longer time than a 90% disinfection with UV only, meaning it only requires a top speed of 3.23 [cm/s]. As computed in the excel table shown Constraint VII, the optimistic cleaning time would be 4.24 [min] for 90% or 8.5 [min] for 99%, which should be within the required 30 [min] (Criterion V) including software overhead time (10 [min]). Hence, we may conclude such mechanical design satisfies both Criterion V and Constraint VII.

LED Params				**Table Size**	(4 person)	
theta	130	deg		W	122	cm
Area_effectiveness	1	cm^2		H	76	cm
# LEDs (Row)	5			A	9272	cm^2
# LEDs (Col)	2					
Radiant Power	10	mW				
				Effectiveness	**Power**	
Goal Energy (x%)	3.5	mJ/cm^2		99%	7	mJ/cm^2
Effectiveness	90%			90%	3.5	mJ/cm^2
N =	10	LEDs				
r =	0.564189584	cm				
h =	0.263085925	cm				
T_period =	0.35	s				
V_spd =	6.447880959	cm/s				
A_per instance Assuming no overlaps	10	cm^2				
t_clean_whole_table =	254.8774117	s	Eqn: A_table / (V_spd * Col * Row * 2r)			
	4.247956862	min				

Figure 3-16. Excel formulation table of optimal conditions with multi-parameters

As Criterion I suggested, the robot should be compact and should not occupy much space from the table-top surface. As Figure 3-17 shows, the current design of the robot (100 [mm] in diameter and 68 [mm] in height) does fit well on a standard 4-person table (1200 [mm] $\times$ 760 [mm]), with occupation ratio of $\eta_{occupation} = \frac{A_{robot}}{A_{table}} = 0.86\%$, which satisfies such criterion.

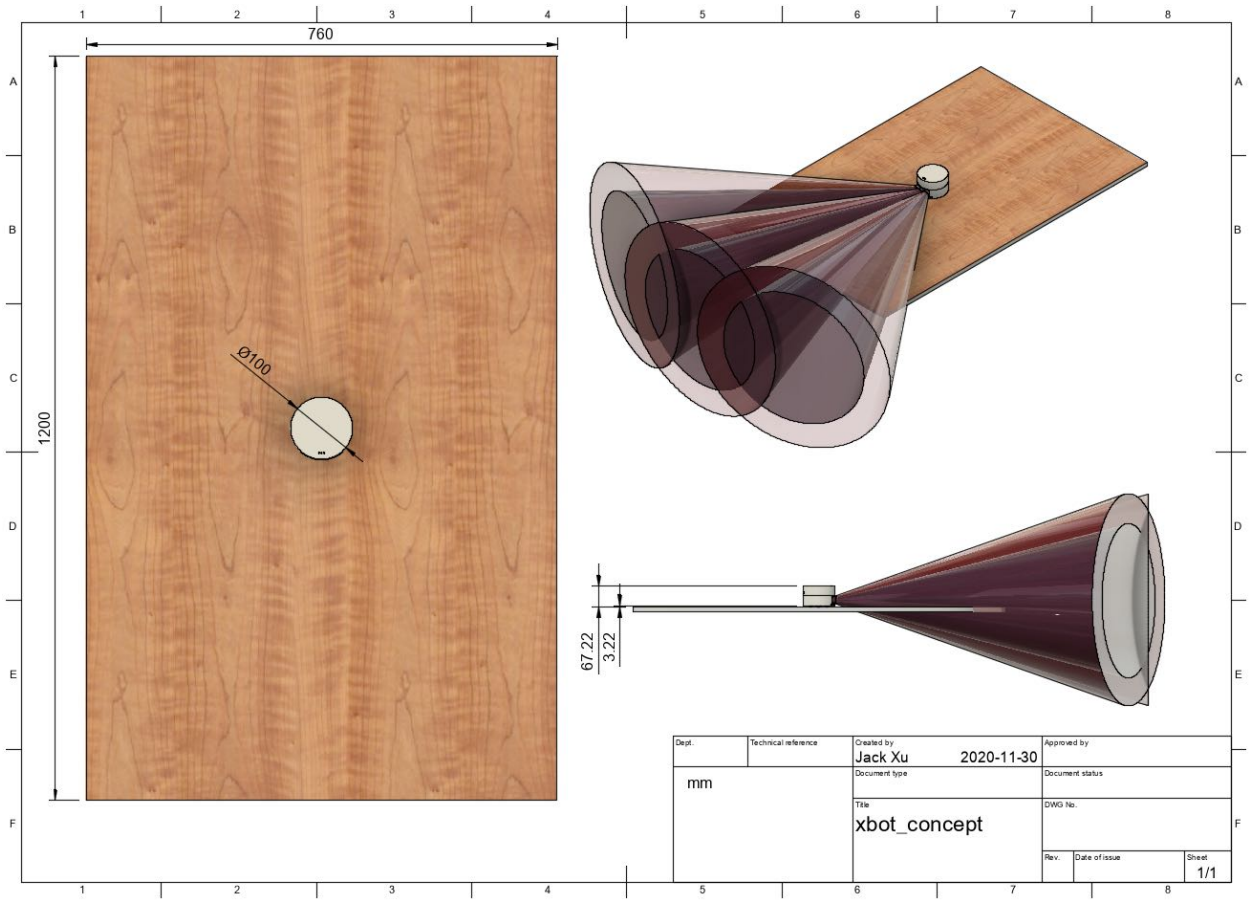

Figure 3-17. Rendered view of the design on a standard 4-person dining table ($120\,[\text{cm}] \times 75\,[\text{cm}]$)

Lastly, as seen in Figure 3-17 and Figure Appendix A-6, the custom Lidar sensor covers a reasonable amount of the table-top regions (and up to 4 meters). To note, the main purpose to adopt the custom ToF sensors as the main method to construct surrounding map is to make the robot low-cost and as low-powered as possible since less data and computation is required for such sensors; in comparison to cameras or Lidar based solutions. In addition, the ToF sensors are robust in most environment including low-light conditions, whereas a camera-based system would struggle (which is a huge factor evaluated by the Criterion III). In contrast, the modern Lidar solution is significantly more expensive (more than 1000 times of the current solution) and overkill, hence, this solution is preferred (as suggested by Constraint V and Criterion IV).

3.2.2 Electrical

Below describes in detail how the electrical system design satisfies the objective and constraints.

To meet the first criteria where the robot must be able to disinfect at least one table of $1.2\,[\text{m}] \times 0.7\,[\text{m}]$ in one charge, a power estimation was calculated to see if the selected battery's capacity can support a full table disinfection. In Figure 3-16, a time estimate to clean a table was calculated based on UV LED performance needs. This time can be used to approximate how long all the electrical components will be running on power for one full cleaning cycle shown in Figure 3-18. Since the UV LEDs and motors draws the most current during the cycle, their power consumption is calculated assuming that they are constantly running for the full duration. Assuming that the highest power consuming UV LED is chosen, if using 10 LEDs rated at 975mW per LED, the total battery capacity used is about 62mAh. With two motors consuming at 1A the battery capacity consumed is about 77mAh. Therefore, in total, the system is estimated to be consuming 138.72mAh per cleaning cycle. Since the battery chosen is 1500mAh, there is a safety factor of about 10.8 to meet the desired criteria. Also note, that if the worst case power consumption estimates are

used where all sensors and actuators are running at max power during the whole duration, the total battery capacity used is still below 1500mAh as shown in Table 3-2.

UV Power Consumption per Table		
Power Dissipation per LED	975	mW
Time to Clean Table	0.070799281	hour
Watt hour	0.069029299	Wh
Battery Voltage	11.1	V
Battery Capacity used per LED	6.218855766	mAh
Number of LEDs	10	LEDs
Total Battery Capacity Used	62.18855766	mAh
Motor Power Consumption per Table		
Current consumption per motor	1	A
Motor Voltage	6	V
Time to Clean Table	0.070799281	hour
Watt hour	0.424795686	Wh
Battery Voltage	11.1	V
Battery Capacity used per Motor	38.26988164	mAh
Number of Motors	2	Motors
Total Battery Capacity Used	76.53976327	mAh
Total Capacity Needed	**138.7283209**	**mAh**

Figure 3-18. Battery Capacity Consumption Calculations

To meet the second criteria where the robot must be able to operate safely on the table top without knocking of objects, an object detection sensor is selected. The VL53L1x ToF sensor will sense obstacles in front of the robot. To increase field of view, three will be used to maximize object detection ability.

To meet the third criteria where the robot must be able to stay on table top without exceeding the table-top boundary, IR sensors were selected in order to send a signal when the robot is at the edge of the table.

To meet the sixth criteria where the robot must pose minimum risk to nearby people (such as UV exposure), IR sensors will be used to detect when a robot is lifted off the the table. This IR sensor signal will then trigger the hardware shutdown circuit for the UV LED drive circuit, as elaborated in Section 3.1.2.6. The simulation result shown in Figure 3-19 displays that the LED current (green) indeed shuts down with IR signal (red) crossing the threshold (light-blue).

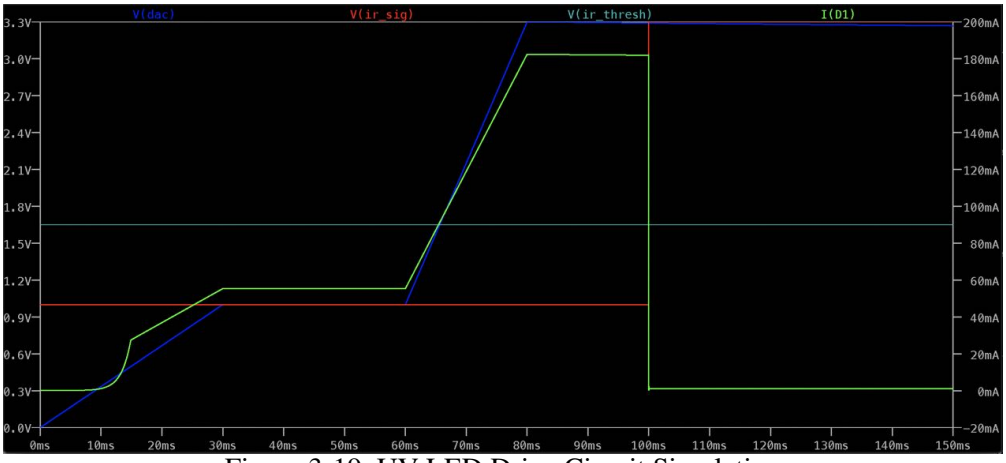

Figure 3-19. UV LED Drive Circuit Simulation

Lastly, to meet the seventh criteria where the robot must be able to sanitize $> 99\%$ of common bacteria and viruses including SARS-CoV-2, research is being performed to model the effectiveness of UV disinfection. There are papers found that can help calculate the disinfection effectiveness based on the UV radiant power per surface area. For example, using a 280nm wavelength UV light on SARS-Cov-2 requires a dose of about $3.75mJ \left[\text{mJ}/\text{cm}^2\right]$ as mentioned in [16]. There is also a partnership with Professor Aucoin who has access to labs that allow testing on common bacteria that will allow further design validation of the UV LED system.

3.2.3 Software

There are certain constraints and criteria that wanted to be met in the software domain. First of all Constraint I requires the robot to generate a complete path from beginning to end that covers the entire surface of the table as quickly as possible. Such a constraint will be achieved by the coverage path planning algorithms which ensure that the path generated completely covers the full surface area. Additionally, the Zig-Zag motion will reduce the total time to completion as it is mentioned in [13]. Future implementations of the algorithm in the simulation can be used to measure the time to completion to ensure that the constraint is met.

Secondly Constraint II can be achieved by implementing a obstacle avoidance algorithm using the known map of the environment as well as the frontal bumper sensors. If a complete map of the environment along with the position of the obstacles is well determined and assuming that the map is static, the coverage path can generate a path that traverses along the map, providing a complete coverage as well as avoiding any obstacles. Additionally, in case of a failure in mapping or localization, the frontal collision sensors can be used to trigger a movement strategy that tries to avoid obstacles that are in front of the robot. The IR sensors placed at the bottom of the robot can also be used to determine the edge of the table and follow along the edge. The IR sensors at the side will allow the robot to follow the edge of the table while the frontal IR sensors will alert the robot when the end of the table is reached; hence achieving Constraint III.

Constraint VII and Criterion II require that while the robot is moving along its predetermined path, the cleaning and disinfection mechanism are active as well. The UV LED arrays and the disinfective fluid will be active as the robot traverses its path, ensuring that the surface it travels along is disinfected.

4 Schedule and Budget

4.1 Schedule

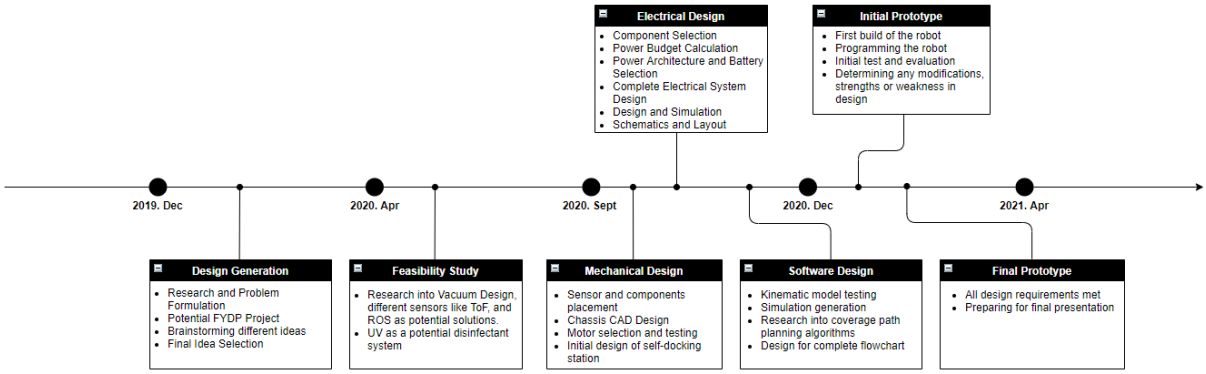

Figure 4-1. Brief Timeline of MTE 481 and MTE 482.

The figure above shows a brief outline of the different milestones for MTE 481 and MTE 482. With MTE 481 coming to an end, here we have outlined some of the key expected schedules for MTE 481.

January $\sim$ February
By these months, we hope to have a fully operating version of the solution. All of the different components will come together during this phase to be tested. This implementation will be thoroughly reviewed to see what is working and what is not to develop further plans of actions. This phase will likely be a repetitive process of testing the solution, finding issues and making changes until settling on a final design. Testing will consist of going back to our problem statement and design criteria, setting up an environment, and recording observations of whether the robot interacts with its surroundings as expected. Using the results from testing, the constraints and criteria can either be relaxed or further improvements and changes can be made to the robot until satisfactory results are achieved.

March $\sim$ April
With the robot fully implemented and no further modifications needed, the team will start working on any additional deliverable that are required for the course (final report, video demonstration, posters, ...).

4.2 Budget, expected costs

The Bill of Material for mechanical and electrical is shown in Figure Appendix D-1 and Figure Appendix D-2, respectively. The summarized table is shown below in Table 4-1.

Table 4-1. BOM summary

Domain	Total Cost (CAD)
Mech Total	68.1
Elec- Sensor Boards	218.38
Elec- MCU Boards	55.76
Elec- Driver Board	14.575
Elec- Power Board	36.78
TOTAL	393.63

The originally proposed budget was to be below $300 CAD, but the current budget is exceeding it by roughly $100 CAD. Looking at the summary table, the cost for sensor boards is much higher than that of other boards in the electrical system. The detailed cost breakdown for sensor boards is shown below.

UVC Sensor	3 pin Connector	6.8
UVC Sensor	UV LED	104.5
UVC Sensor	3 pin cable, len: 152mm	17.4
IR sensor breakout	3 pin cable, len: 152mm	10.44
IR sensor breakout	IR sensor breakout	22.68
ToF sensor breakout	ToF sensor breakout	42.21
ToF sensor breakout	6 pin cable, len: 0152mm	6.57
Collision Sensor	ESE-22MH24	2.56
Collision Sensor	3 pin cable, len: 152mm	5.22

Figure 4-2. Detailed Sensor Board Cost Breakdown

The most expensive item here is the UV LED. Currently, the UV LED is selected based on the highest power dissipation since its effectiveness to virus has not been tested yet. This was suppose to be tested in early stage with help from Professor Aucoin, but due to COVID, entering his lab became difficult and hence has not been tested yet. Thus in the design, the highest power dissipating LED is selected which is the most expensive one. Additionally, the number of LED is currently set as 10, and again after testing this potentially can be reduced too. Using the lowest power dissipation UV LED available and reducing the LED number by half, the LED cost will be $25 CAD. This will reduce the total cost to $325 CAD which is closer to the originally proposed budget. Nevertheless, the expected budget needs to be increased, and the exact amount depends on the result of the UV LED testing.

5 Conclusions and recommendations

Overall, the design thus far is able to meet most of the constraints and criteria that has been set at the beginning of the FYDP. Starting off with constraints, the robot is expected to disinfect a standard table in one charge with a combination of the UV LEDs, the piezo disinfectant sprayer and the motors; all of which are estimated to consume less capacity than a full battery. The robot is expected to detect obstacles and maneuver around them accordingly by utilizing the ToF sensor, bumper sensor, appropriate mapping, and localization. The robot should stay within the tabletop boundaries with the help of IR sensors to detect the edge. The robot is expected to support the appropriate load as proven in motor load calculations. Even if the predicted budget being a quite strict, there are still evident improvements to be made that can ensure the cost of production is cheap enough to be considered viable on the market. Lastly, the robot is predicted to be able to sanitize bacteria at 99% with support from research paper claims and the assistance of Professor Aucoin.

For criteria, the selection of components have always had total size in mind, from the battery to motors and the design of the chassis. To cover as much surface area as possible, a battery is chosen to go above and beyond the necessary capacity needed to clean a standard table on a single charge. To be adaptable to various environments, path planning, mapping, and localization methods were considered to gain confidence in many environmental edge cases. Lastly, as shown throughout the report, cost and robot performance is always optimized in all stages of design.

Even with all the precautions in place, there are still uncertainties about the predicted performance of the project. Disinfection ability can only be truly verified once the UV disinfection system is tested in lab which has been delayed due to recent COVID-19 outbreaks. It is recommended to keep in touch with the Professor to look for more opportunities to work in the Lab in the upcoming term. Cost of the project will need to decrease in order to safely meet constraints which will require more thought on the necessity of certain components such as the UV LED system. It is recommended to go through the Bill of Materials once again to see if there are any obvious cost improvements that can be made. Lastly, robot firmware and software implementation can only be designed and improved with confidence using proper real world verification. Therefore, the prototyping of the system should be accelerated as soon as possible.

All in all, the progress of the FYDP project is in a good place at the end of MTE 481. With the timelines clear, finishing up development, testing, and refining the end product should be feasible by the end of MTE 482 in the winter term.

6 Teamwork Effort

Jianxiang (Jack) Xu:

- Early prototyping and feasibility study
- Mechanical components selection and testing
- Mechanical design in CAD
- Overall sensor selections and concept sketch
- Presentation slides and final report
- Software architecture design and preliminary brainstorming
- Preliminary system design and scope

Tsugumi Murata:

- VL53L1x (ToF) feasibility study
- Electrical component selection and system diagram design
- Component SPICE modelling
- Circuit Design SPICE Simulation
- Component CAD Library Design
- Preliminary Circuit Schematic and Layout Design
- Presentation slides and final report

Jerome Villapando:

- Professor partnership relations
- Electrical design research
- Electrical component testing and feasibility
- Early MCU communication prototyping
- Electrical component selection and system diagram design
- Presentation slides and final report

Dong Jae (Alex) Park:

- Presentation slides and final report
- Software architecture design and preliminary brainstorming
- Kinematic motion modelling of robot in MATLAB
- Initial set-up of simulation environment in Webots
- Early research into different motion planning methodologies

Glossary

CAD Computer-Aided Design.
COVID Coronavirus.

DAC Digital-to-Analog Converter.

ESP32 ESP32.

FYDP Fourth Year Design Project.

IMU Inertial measurement unit.
IR Infrared.

LED Light Emitting Diode.
Lidar Lidar, which stands for Light Detection and Ranging.

MCU Micro-controller Unit.

OTA Over the air.

PCB Printed Circuit Board.

ROI Region of Interest.
Roomba Roomba Robot.
RPM Rate per minute.

SLAM Simultaneous Localization and Mapping.
SPICE Simulation Program with Integrated Circuit Emphasis.

ToF Time of Flight.

UV Ultra-violet.

References

[1] *Antibiotic resistance threats in the united states*. [Online]. Available: https://stacks.cdc.gov/view/cdc/82532.

[2] G. o. C. News, *Coronavirus disease (covid-19): Summary of assumptions*, 2020. [Online]. Available: https://www.canada.ca/en/public-health/services/diseases/2019-novel-coronavirus-infection/health-professionals/assumptions.html.

[3] L. A. T. News, *$160,000 to buy germ zapping robot for langley hospital*, 2020. [Online]. Available: https://www.langleyadvancetimes.com/community/160000-to-buy-germ-zapping-robot-for-langley-hospital/.

[4] R. News, *Scientists develop ultraviolet drone to fight covid-19*, 2020. [Online]. Available: https://www.rte.ie/news/business/2020/0603/1145178-scientists-develop-ultraviolet-drone-to-fight-covid-19/.

[5] *Vl53l1x time-of-flight distance sensor carrier with voltage regulator, 400cm max*. [Online]. Available: https://www.pololu.com/product/3415.

[6] Hai Prasaath K, *Choosing batteries for robots*. [Online]. Available: https://www.engineersgarage.com/egblog/choosing-battery-for-robots/.

[7] *Goldbat 1500mah 11.1v 100c 3s lipo battery with xt60 connector for uav fpv racing drone mini*. [Online]. Available: https://www.amazon.ca/GOLDBAT-1500mAh-Battery-Connector-Racing/dp/B07P2WBRDJ/ref=pd_sbs_21_1/137-4621262-5205211?_encoding=UTF8&pd_rd_i=B07P2WBRDJ&pd_rd_r=489bda1d-7b32-4ace-96af-ae324f230368&pd_rd_w=qAScm&pd_rd_wg=YdFBU&pf_rd_p=0344dcd7-676a-4f7e-bc24-9ae78fa8eca2&pf_rd_r=V490BXN3VZNDB5CM00D9&psc=1&refRID=V490BXN3VZNDB5CM00D9.

[8] *Esp32-wroom-32e*. [Online]. Available: https://www.espressif.com/sites/default/files/documentation/esp32-wroom-32e_esp32-wroom-32ue_datasheet_en.pdf.

[9] *World's lowest power 9-axis mems motiontracking™ device*. [Online]. Available: https://cdn.sparkfun.com/assets/7/f/e/c/d/DS-000189-ICM-20948-v1.3.pdf.

[10] *Sparkfun line sensor breakout - qre1113 (analog)*. [Online]. Available: https://www.sparkfun.com/products/9453.

[11] *Ltspice*. [Online]. Available: https://www.analog.com/en/design-center/design-tools-and-calculators/ltspice-simulator.html.

[12] *2 pack ultrasonic atomization maker 20mm 113khz mist atomizer diy humidifier with pcb 3.7-12v*. [Online]. Available: https://www.amazon.ca/Ultrasonic-Atomization-Atomizer-Humidifier-3-7-12V/dp/B07V9GF44J/ref=pd_bxgy_img_2/137-4621262-5205211?_encoding=UTF8&pd_rd_i=B07V9GF44J&pd_rd_r=dda4d519-7a3e-43bb-87e2-c990bbfa5a64&pd_rd_w=v8hVk&pd_rd_wg=PnjOA&pf_rd_p=42339929-297e-4141-b7b2-fe55db70f4b7&pf_rd_r=E9C4J9RNCFA6JXC2Z0F5&psc=1&refRID=E9C4J9RNCFA6JXC2Z0F5.

[13] S. Kim, ''Ieee international conference on robotics and automation, 2004. proceedings. icra '04. 2004,'' vol. 5, pp. 4437–4441, 2004. DOI: 10.1109/ROBOT.2004.1302416.

[14] M. S. C. T. Mathworks-Robotics, *Mathworks-robotics/mobile-robotics-simulation-toolbox*. [Online]. Available: https://github.com/mathworks-robotics/mobile-robotics-simulation-toolbox.

[15] *75:1 micro metal gearmotor hp 6v*. [Online]. Available: https://www.pololu.com/product/2361.

[16] Y. Gerchman, *Uv-led disinfection of coronavirus: Wavelength effect*, 2020. [Online]. Available: https://www.researchgate.net/publication/344286694_UV-LED_disinfection_of_Coronavirus_wavelength_effect_1_2.

Appendix A More Detailed Views of the Mechanical CAD Models

Figure Appendix A-1. Preview render of the robot

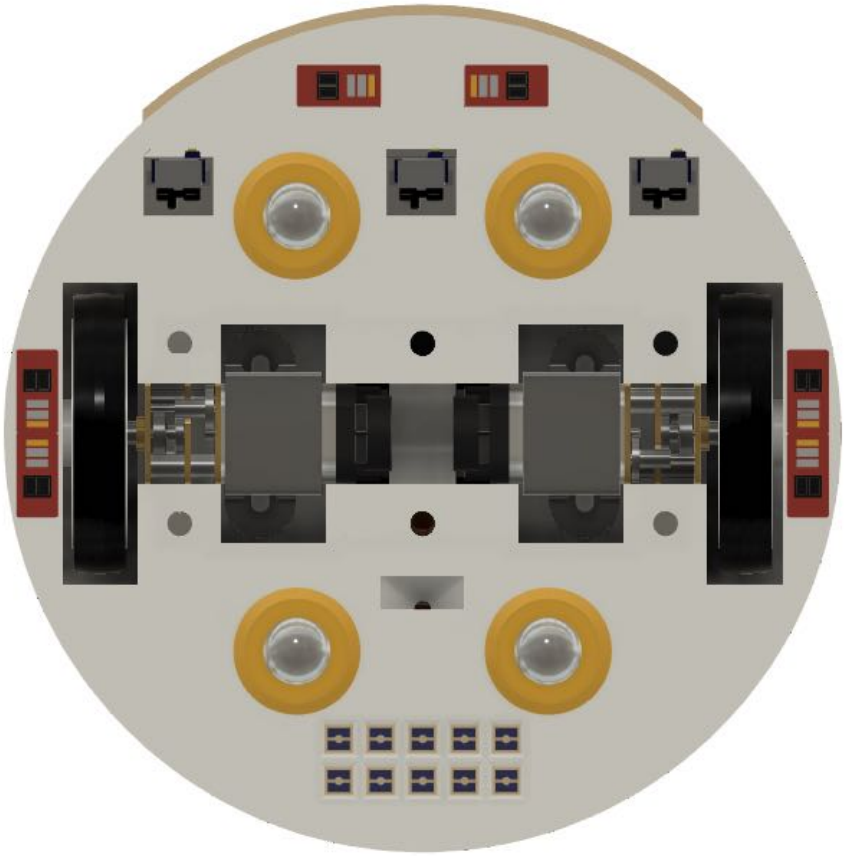

Figure Appendix A-2. Bottom view of the robot

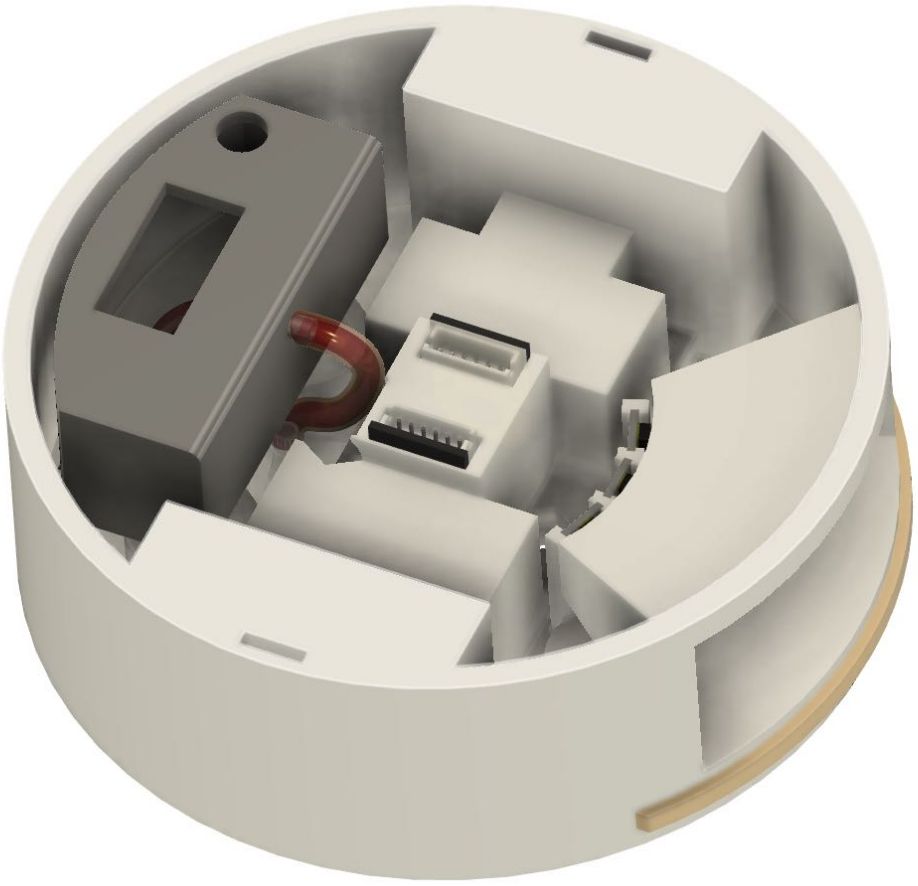

Figure Appendix A-3. Orthogonal view of the bottom chassis

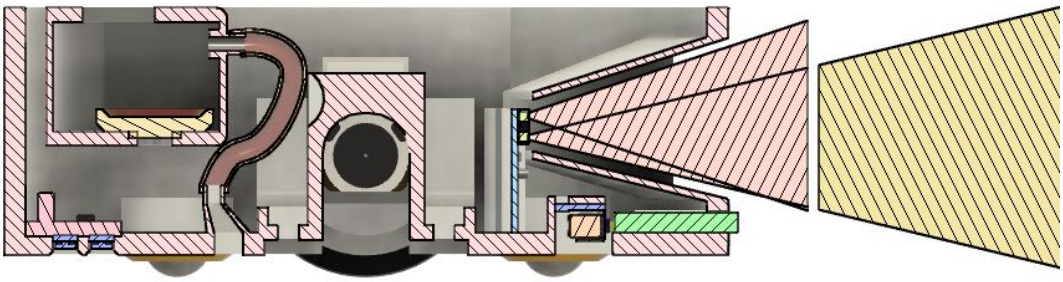

Figure Appendix A-4. Cross-section view of the bottom chassis

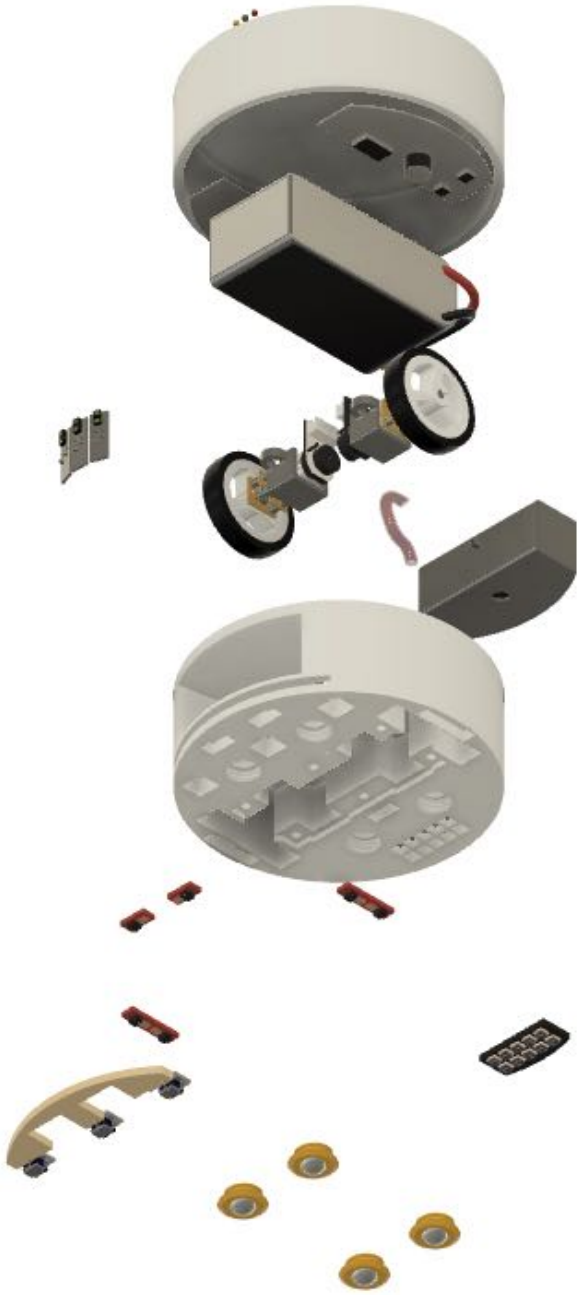

Figure Appendix A-5. Explode view of the robot

Figure Appendix A-6. ToF Coverage view of the robot on a table-top

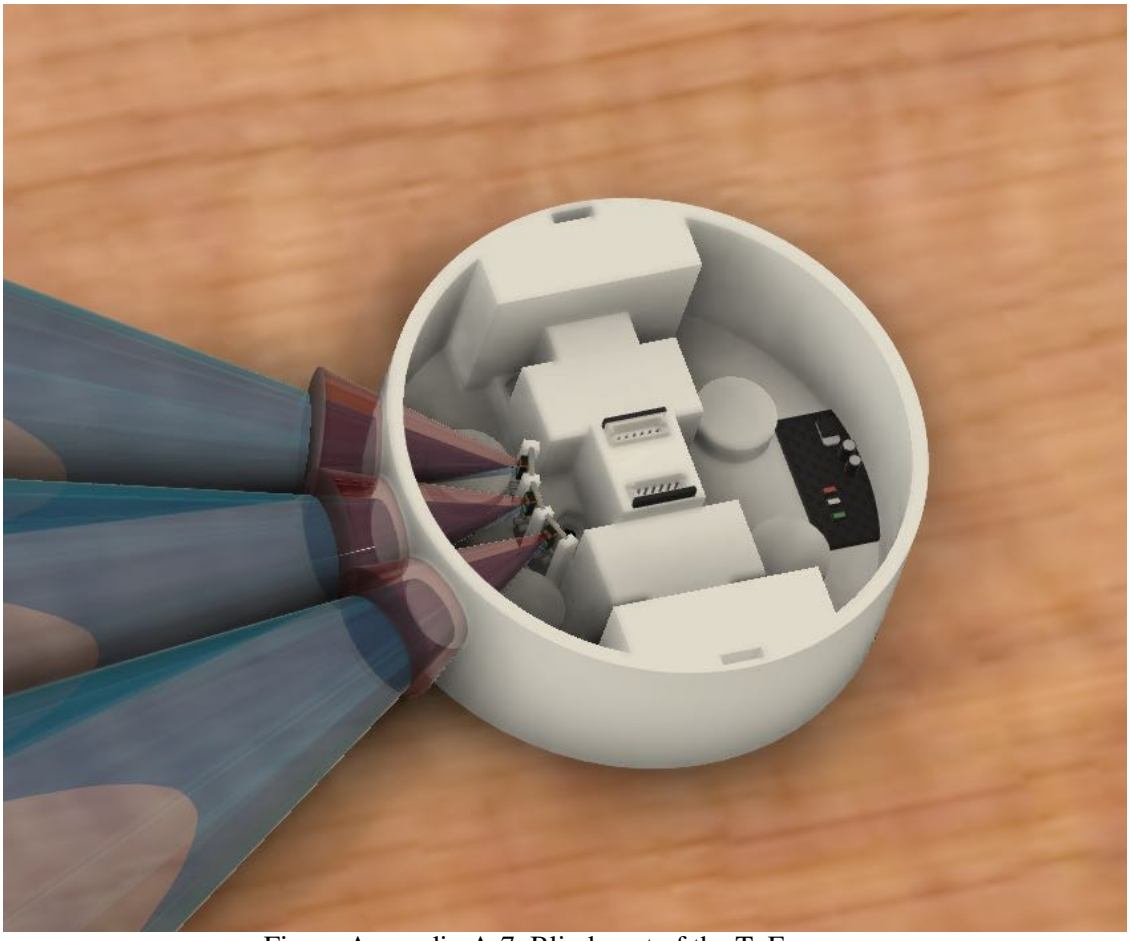

Figure Appendix A-7. Blind-spot of the ToF sensor

Appendix B Electrical Appendix

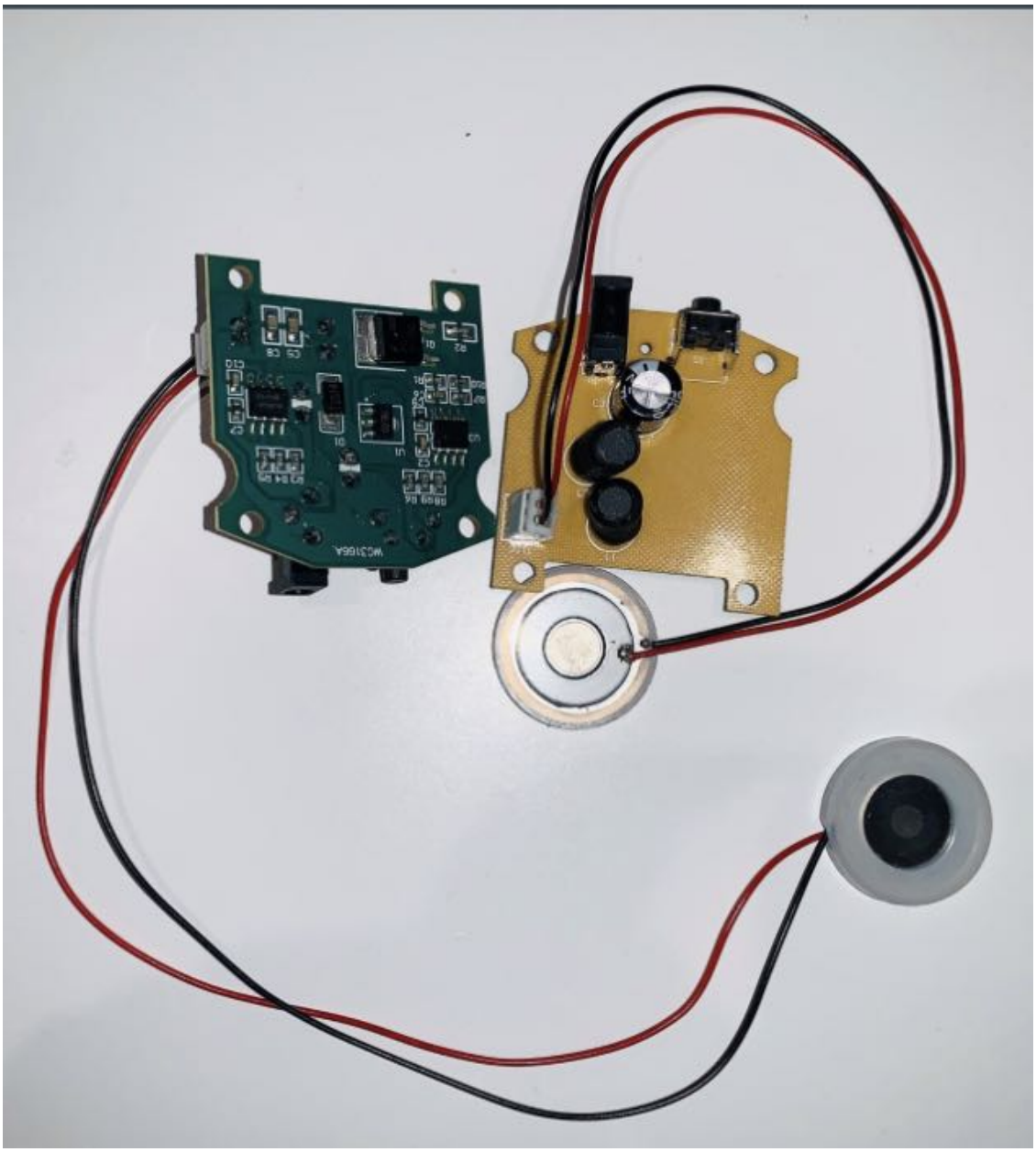

Figure Appendix B-1. Piezo Drive Circuit used for PoC

Appendix C Excel/Calculation Table

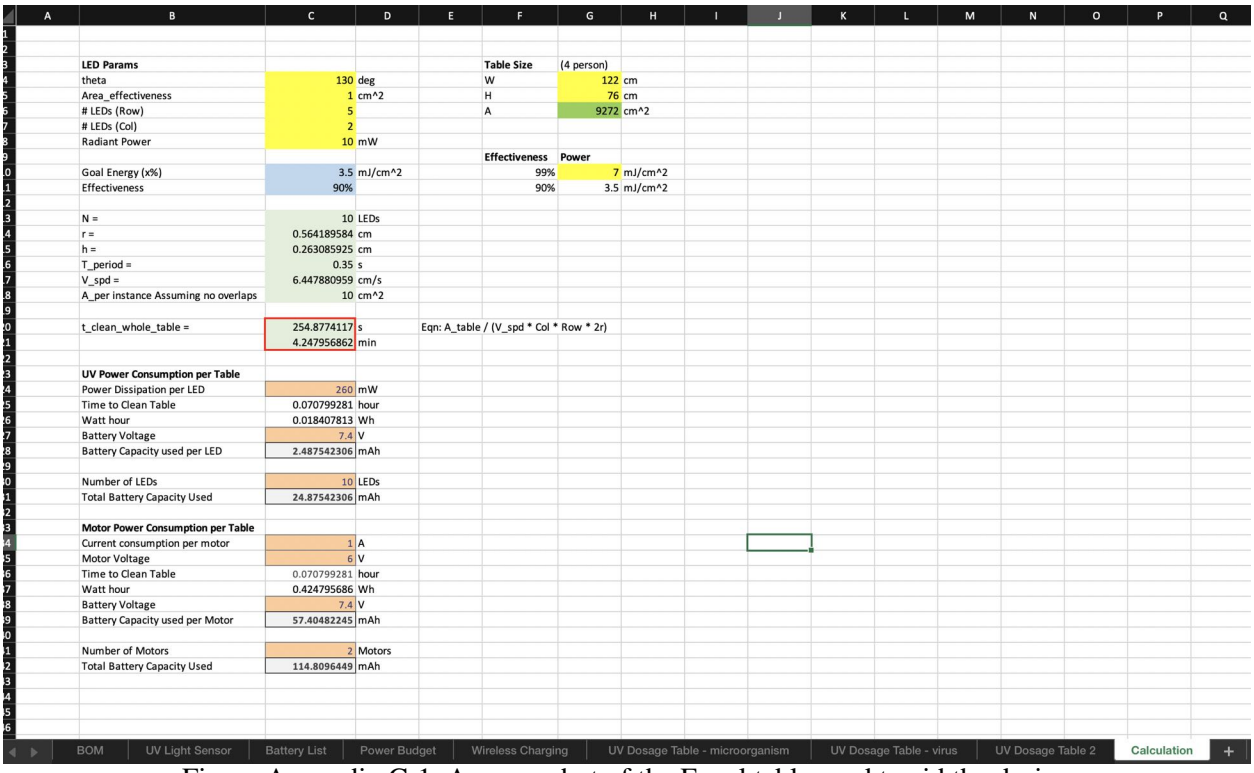

	A	B	C	D	E	F	G	H	I	J	K	L	M	N	O	P	Q
1																	
2																	
3		**LED Params**				**Table Size**	(4 person)										
4		theta	130	deg		W	122	cm									
5		Area_effectiveness	1	cm^2		H	76	cm									
6		# LEDs (Row)	5			A	9272	cm^2									
7		# LEDs (Col)	2														
8		Radiant Power	10	mW													
9						**Effectiveness**	**Power**										
10		Goal Energy (x%)	3.5	mJ/cm^2		99%	7	mJ/cm^2									
11		Effectiveness	90%			90%	3.5	mJ/cm^2									
12																	
13		N =	10	LEDs													
14		r =	0.564189584	cm													
15		h =	0.263085925	cm													
16		T_period =	0.35	s													
17		V_spd =	6.447880959	cm/s													
18		A_per instance Assuming no overlaps	10	cm^2													
19																	
20		t_clean_whole_table =	254.8774117	s	Eqn: A_table / (V_spd * Col * Row * 2r)												
21			4.247956862	min													
22																	
23		**UV Power Consumption per Table**															
24		Power Dissipation per LED	260	mW													
25		Time to Clean Table	0.070799281	hour													
26		Watt hour	0.018407813	Wh													
27		Battery Voltage	7.4	V													
28		Battery Capacity used per LED	2.487542306	mAh													
29																	
30		Number of LEDs	10	LEDs													
31		Total Battery Capacity Used	24.87542306	mAh													
32																	
33		**Motor Power Consumption per Table**															
34		Current consumption per motor	1	A													
35		Motor Voltage	6	V													
36		Time to Clean Table	0.070799281	hour													
37		Watt hour	0.424795686	Wh													
38		Battery Voltage	7.4	V													
39		Battery Capacity used per Motor	57.40482245	mAh													
40																	
41		Number of Motors	2	Motors													
42		Total Battery Capacity Used	114.8096449	mAh													
43																	
44																	
45																	
46																	

BOM | UV Light Sensor | Battery List | Power Budget | Wireless Charging | UV Dosage Table - microorganism | UV Dosage Table - virus | UV Dosage Table 2 | Calculation | +

Figure Appendix C-1. A screenshot of the Excel table used to aid the design

	Component	Description	Designator	Continuous Operation	Sleep / Off load Current Consumption (mA)	Nominal Current Consumption (mA)	Maximum Current Consumption (mA)	Note	Datasheet
3.3V	ESP32	MCU / WiFi		Yes	0.8	630	740	*Wifi TX @ 0dB + minimum operating MCU voltageused for Nominal	https://www.espressif.com/sites/defa
	VL53L1X	ToF sensor		50hz	0.009	16	18	*Operating current-> Ranging average	https://www.st.com/resource/en/data
	VL53L1X	ToF sensor		50hz	0.009	16	18	*Operating current-> Ranging average	https://www.st.com/resource/en/data
	VL53L1X	ToF sensor		50hz	0.009	16	18	*Operating current-> Ranging average	https://www.st.com/resource/en/data
	ICM-20948	IMU sensor			0.008	3.11	3.11	*Operating current->9-Axis (DMP disabled)	https://cdn.sparkfun.com/assets/7/f/e
	QRE1113	IR sensor			0	70	70	*Used absolute max ratings for operating voltage	https://www.sparkfun.com/products/
	QRE1113	IR sensor			0	70	70	*Used absolute max ratings for operating voltage	
	QRE1113	IR sensor			0	70	70	*Used absolute max ratings for operating voltage	
	QRE1113	IR sensor			0	70	70	*Used absolute max ratings for operating voltage	
	QRE1113	IR sensor			0	70	70	*Used absolute max ratings for operating voltage	
	QRE1113	IR sensor			0	70	70	*Used absolute max ratings for operating voltage	
EXACT SUM					0.835	1101.11	1217.11		
10% PAD					0.9185	1211.221	1338.821		

	Component	Description	Designator	Continuous Operation	Sleep / Off load Current Cpnsumption	Nominal Current Consumptic	Maximum Current Consumption (mA)	Note	
6V	Motors	DC motor				1000	1000	*since low rpm, using stall current as reference	https://optoelectronics.liteon.com/up
	Motors	DC motor				1000	1000	*since low rpm, using stall current as reference	https://www.handsontec.com/datasp
	Vaporizer	Piezo Actuator			20	416.6666667	416.6666667	*Calc assumption made based on data 2.5W from https://www.youtube.com/watch?v=OOZi3QnnDCo	https://www.amazon.ca/Bestol-Ultras
EXACT SUM					20	2416.666667	2416.666667		
10% PAD					22	2658.333333	2658.333333		

	Component	Description	Designator	Continuous Operation	Cpnsumption (mA)	Consumption (mA)	Maximum Current Consumption (mA)	Note	
10V	LTPL-G35UV275GR-E	UVC LED		PWM, duty TBD	0	20	150		
	LTPL-G35UV275GR-E	UVC LED		PWM, duty TBD	0	20	150		
	LTPL-G35UV275GR-E	UVC LED		PWM, duty TBD	0	20	150		
	LTPL-G35UV275GR-E	UVC LED		PWM, duty TBD	0	20	150		
	LTPL-G35UV275GR-E	UVC LED		PWM, duty TBD	0	20	150		
	LTPL-G35UV275GR-E	UVC LED		PWM, duty TBD	0	20	150		
	LTPL-G35UV275GR-E	UVC LED		PWM, duty TBD	0	20	150		
	LTPL-G35UV275GR-E	UVC LED		PWM, duty TBD	0	20	150		
	LTPL-G35UV275GR-E	UVC LED		PWM, duty TBD	0	20	150		
	LTPL-G35UV275GR-E	UVC LED		PWM, duty TBD	0	20	150		
EXACT SUM					0	200	1500		
10% PAD					0	220	1650		

	Component	Description	Designator	Continuous Operation	Sleep / Off load Current Cpnsumption	Nominal Current Consumptic	Maximum Current Consumption (mA)	Note	
24V	Vaporizer	Piezo Actuator			10.81081081	225.2252252	225.2252252	*Calc assumption made based on data 2.5W from https://www.youtube.com/watch?v=OOZi3QnnDCo	https://www.amazon.ca/Bestol-Ultras
EXACT SUM					10.81081081	225.2252252	225.2252252		
10% PAD					11.89189189	247.7477477	247.7477477		

Figure Appendix C-2. Power Budget

Battery Name	Manufacture	Battery Config	Battery Material	Nominal Voltage (V)	Max Voltage (V)	Capacity (mAh)	Discharge Capacity	Battery Life	PTC?	Cost (CAD)	Unit Cost (CAD)	Size
eneloop	Panasonic	1 cell	Ni-MH	1.2	1.5	2000	1	2100 rechargable	Yes, temperature protection circuit	55.99 (for 16)		3.499375 AA (diameter: 14.5mm, length: 50.5mm)
eneloop Pro	Panasonic	1 cell	Ni-MH	1.2	1.5	2550	1	500 rechargable	Yes, temperature protection circuit	76.68 (for 12)		6.390833333 AA (diameter: 14.5mm, length: 50.5mm)
Amazon Basic AA	Amazon	1 cell	Ni-MH	1.2	1.5	2000		1000 rechargable	over-voltage protection	34.94 (for 16)		2.18375 AA (diameter: 14.5mm, length: 50.5mm)
LITHIUM ION POLYMER BATTERY - 3.7V 2500MAH	Elmwood	1 cell	Li-ion	3.7	4.2	2500			included protection circuitry keeps the battery voltage from goir	23.99	23.99	47mm x 61mm x 6.7mm
LITHIUM ION CYLINDRICAL BATTERY - 3.7V 2200MAH	Elmwood	1 cell	Li-ion	3.7	4.2	2200			over-voltage, under-voltage and over-current protection	15.99	15.99	69mm x Diameter18mm
LITHIUM ION BATTERY PACK - 3.7V 6600MAH	Elmwood	1 cell	Li-ion	3.7	4.2	6600			over-voltage, under-voltage and over-current protection	49.99	49.99	69mm x 54mm x 18mm
LITHIUM ION BATTERY PACK - 3.7V 4400MAH	Elmwood	1 cell	Li-ion	3.7	4.2	4400			over-voltage, under-voltage and over-current protection	32.99	32.99	69mm x 37mm x 18mm
7.2V AA Battery Pack 1500mAh with wire leads	Canadian Batteries	6 cell	Ni-MH	7.2		1500				30.74	30.74	84.65 x 51.42 x 14.50 mm
12V 6/5A NiMh Battery Pack 3800Mah with wire leads	Canadian Batteries	10 cell	Ni-MH	11.1	12.6	3800				55.45	55.45	84.80 x 69.80 x 34.20 mm
Lipo 7.2v 800mAh 30C		2 cell	Li-Po	11.1	12.6	800	30					58 x 15 x 30 mm
Lipo 12v 1500mAh		3 cell	Li-Po	11.1	12.6	1500						
Lipo 3. 7V 800mAh 25C		1 cell	Li-Po	3.7	4.2	800	25					40 x 25 x 9 mm
Lipo 11. 1V 1500mAh 100C	Goldbat	3S1P	Li-Po	11.1	12.6	1500	100			25.99	25.99	72 x 35 x 26 mm

Figure Appendix C-3. Battery Candidate List

Battery

Battery	Battery Nominal Voltage	Battery Max Voltage	Capacity	Material	Discharge Capacity
Lipo 11.1V 1500mAh 100C	11.1	12.6	1500	Li-Po	100

Total Battery Current Consumption (approx)

Enable	Rail (V)	Rail Max Current (mA)	Rail 10% PAD max current (mA)	Regulation Mode	output power (W)	source voltage (V)	approx efficiency	source current (mA)
	11.1	225.2252252	247.7477477	direct feed	2.75	11.1	0.99	0
o	10	1500	1650	Buck	16.5	11.1	0.9	1651.651652
o	3.3	1217.11	1338.821	Buck	4.4181093	11.1	0.9	442.2531832
o	6	2000	2200	Buck	13.2	11.1	0.9	1321.321321
o	24	225.2252252	247.7477477	Boost	5.945945946	11.1	0.9	595.1897844
							total approx source current	4010.415941
							Operation _time (min)	10
							Operation _time (hour)	0.166666667
							Operation Battery consumption(mAh)	668.4026568
							Required Dsicharge Capacity	2.673610627

Figure Appendix C-4. Battery Consumption Calculation

Appendix D   BOM Table

Mechanical								
Group	Part	Vendor	Price	Dimension	Quantity Per Robot	Quantity to Order	total Cost	Link
Ball Caster	DFRobot 0.4" Ball Caster with Metal Ball	Robotshop	$2.53		2	2	5.06	https://www.robotshop.com/en/dfrobot-ba
	Rotation Caster 5/8 Inch 33 lbs Roller Ball Bearings(5p	Amazon	$14.99		0.5	1	7.495	https://www.amazon.ca/Transfer-KangTeer-I
	Ball Transfer Unit KangTeer 10pcs Universal Base Meta	Amazon	$19.89	Ball Diam: 15mm/0.6"; Total Size: 24 x 30mm/0.9" x 1"(H*D)	0.2	1	3.978	https://www.amazon.ca/Transfer-KangTeer-U
	UOTYLE 5/8 Ball Transfer Unit Bearing 22Lb Casters Ro	Amazon	$21.22		0.33	1	7.0026	https://www.amazon.ca/UOTYLE-Transfer-Be
Ball Caster (custom)	1/4" bearing ball x100	Amazon	$6.99		0.02	1	0.1398	https://www.amazon.ca/HFS-Pieces-Bracket-
	1" bearing ball x10	Amazon	$15.99		0.2	1	3.198	https://www.amazon.ca/HFS-Package-Chron
	1/2" bearing ball x100	Amazon	$20.95		0.02	1	0.419	https://www.amazon.ca/Avler-AV12SA-Calib
motor	75:1 Micro Metal Gearmotor HP 6V	Pololu	$20.42		2	2	40.84	https://www.pololu.com/product/2361
Mech Toal							68.1324	

Figure Appendix D-1. Mech BOM

Electrical										
Board	Component	Part Name	Digikey Part Number	Unit Price	Description	Quanitity per board	Quanity per Robot	Quanitity to Order (margin)	Total Cost	LINK
UVC Sensor	3 pin Connector	SM03B-SRSS-TB(LF)(SN)	455-1803-1-ND	0.68	Connector Header Surface Mount, Right Angle 3 position 0.039" (1.00mm)	1	10	10	6.8	https://www.digikey.ca/en/products/detail/jst-s
UVC Sensor	UV LED	LTPL-G35UV275GR-E	160-LTPL-G35UV275GR-ECT-ND	10.45	Ultraviolet (UV) Emitter 277nm 7.2V 200mA 120°	1	10	10	104.5	https://www.digikey.ca/en/products/detail/lite-
UVC Sensor	3 pin cable, len: 152mm	A03SR03SR30K152A	455-3703-ND	1.74	3 Position Cable Assembly Rectangular Socket to Socket, Reversed 0.500' (152.40m	1	10	10	17.4	https://www.digikey.ca/en/products/detail/jst-s
MCU Board (UVC Driver)	3 pin Connector	SM03B-SRSS-TB(LF)(SN)	455-1803-1-ND	0.68	Connector Header Surface Mount, Right Angle 3 position 0.039" (1.00mm)	1	10	10	6.8	https://www.digikey.ca/en/products/detail/jst-s
MCU Board (UVC Driver)	Op-amp	LMV358AIDR	296-47593-1-ND	0.71	General Purpose Amplifier 2 Circuit Rail-to-Rail 8-SOIC	7	7	7	4.97	https://www.digikey.ca/en/products/detail/texa
MCU Board (UVC Driver)	BJT	DMMT5551-7-F	DMMT5551-FDICT-ND	0.62	Bipolar (BJT) Transistor Array 2 NPN (Dual) Matched Pair 160V 200mA 300MHz 30	7	7	7	4.34	https://www.digikey.ca/en/products/detail/dioc
MCU Board	MCU	ESP32-DEVKITC-32D-F	1965-1003-ND	15.07	Transceiver; 802.11 b/g/n (Wi-Fi, WiFi, WLAN), Bluetooth® Smart Ready 4.x Dual Mo	1	1	1	15.07	https://www.digikey.ca/en/products/detail/esp
MCU IMU Sensor	IMU	ICM-20948	1428-1123-1-ND	11.02	Accelerometer, Gyroscope, Magnetometer, 9 Axis Sensor I^2C, SPI Output	1	1	1	11.02	https://www.digikey.ca/en/products/detail/tdk-
MCU Board (IR)	3 pin Connector	SM03B-SRSS-TB(LF)(SN)	455-1803-1-ND	0.68	Connector Header Surface Mount, Right Angle 3 position 0.039" (1.00mm)	6	6	6	4.08	https://www.digikey.ca/en/products/detail/jst-s
MCU Board (ToF)	6 pin Connector	SM06B-SRSS-TB(LF)(SN)	455-1806-1-ND	1.08	Connector Header Surface Mount, Right Angle 6 position 0.039" (1.00mm)	3	3	3	3.24	https://www.digikey.ca/en/products/detail/jst-s
MCU Board (Collision)	3 pin Connector	SM03B-SRSS-TB(LF)(SN)	455-1803-1-ND	0.68	Connector Header Surface Mount, Right Angle 3 position 0.039" (1.00mm)	6	6	6	4.08	https://www.digikey.ca/en/products/detail/jst-s
MCU Board (Encoder)	6 pin Connector	SM06B-SRSS-TB(LF)(SN)	455-1806-1-ND	1.08	Connector Header Surface Mount, Right Angle 6 position 0.039" (1.00mm)	2	2	2	2.16	https://www.digikey.ca/en/products/detail/jst-s
Driver Board (Haptic Driver)	piezo actuator			15.33	Bestol 5PCS 16mm Ultrasonic Mist Maker Fogger Discs with Wire & Sealing R	1	1	1	2.555	https://www.amazon.ca/Bestol-Ultrasonic-Fogg
Driver Board (Haptic Driver)	555 Timer	NE555S-13	NE555S-13DICT-ND	0.55	555 Type, Timer/Oscillator (Single) IC 500kHz 8-SO	1	1	2	1.1	https://www.diodes.com/assets/Datasheets/NE
Driver Board (Haptic Driver)	Gate Driver	TC4428ACOA	TC4428ACOA-ND	1.73	1.5A Dual High-Speed Power MOSFET DriversLow-Side Gate Driver IC 8-SOIC	1	1	2	3.46	https://ww1.microchip.com/downloads/en/De
Driver Board (Motor Driver IC)	H bridge IC	DRV8835DSSR	296-30391-1-ND	2.23	IC MTR DRVR BIPOLAR 2-7V 12WSON	1	1	1	2.23	https://www.digikey.ca/en/products/detail/texa
Driver Board (Encoder)	6 pin Connector	SM06B-SRSS-TB(LF)(SN)	455-1806-1-ND	1.08	Connector Header Surface Mount, Right Angle 6 position 0.039" (1.00mm)	2	2	2	2.16	https://www.digikey.ca/en/products/detail/jst-s
Driver Board (buck)	Buck IC 3A	TPS54331GDR	296-50099-1-ND	2.41	IC REG BUCK ADJUSTABLE 3A 8SOIC	1	1	1	2.41	https://www.digikey.ca/en/products/detail/texa
Driver Board (boost)	Boost	MC34063ADR	296-17765-1-ND	0.66	IC REG BUCK BST ADJ 1.5A 8SOIC	1	1	1	0.66	https://www.digikey.ca/en/products/detail/texa
IR sensor breakout	3 pin cable, len: 152mm	A03SR03SR30K152A	455-3703-ND	1.74	3 Position Cable Assembly Rectangular Socket to Socket, Reversed 0.500' (152.40m	6	6	6	10.44	https://www.digikey.ca/en/products/detail/jst-s
IR sensor breakout	IR sensor breakout	QRE1113 (ANALOG)CSV/	Pololu	3.78	SparkFun Line Sensor Breakout - QRE1113 (Analog)	6	6	6	22.68	https://www.sparkfun.com/products/9453
ToF sensor breakout	ToF sensor breakout	VL53L1X	pololu	14.07	VL53L1X Time-of-Flight Distance Sensor Carrier with Voltage Regulator, 400cm Max	3	3	3	42.21	https://www.pololu.com/product/3415
ToF sensor breakout	6 pin cable, len: 0152mm	A06SR06SR30K152B	455-3015-ND	2.19	6 Position Cable Assembly Rectangular Socket to Socket 0.500' (152.40mm, 6.00")	3	3	3	6.57	https://www.digikey.ca/en/products/detail/jst-s
Collision Sensor	ESE-22MH24	ESE-22MH24	P13584SCT-ND	0.64	SWITCH DETECTOR SPST-NO 10MA 5V	4	4	4	2.56	https://www.digikey.ca/en/products/detail/pan
Collision Sensor	3 pin cable, len: 152mm	A03SR03SR30K152A	455-3703-ND	1.74	3 Position Cable Assembly Rectangular Socket to Socket, Reversed 0.500' (152.40m	3	3	3	5.22	https://www.digikey.ca/en/products/detail/jst-s
									0	
Lipo 11.1V 1500mAh 100C	Battery			25.99	GOLDBAT 1500mAh 11.1V 100C 3S Lipo Battery with XT60 Connector for UAV FPV	1	1	1	25.99	https://www.amazon.ca/GOLDBAT-1500mAh-B
Power Board	BQ24171RGYR	BQ24171RGYR	296-41205-1-ND	5.97	Charger IC Lithium Ion/Polymer 24-VQFN (5.5x3.5)	1	1	1	5.97	https://www.digikey.ca/en/products/detail/texa
Driver Board (buck)	Buck IC 3A	TPS54331GDR	296-50099-1-ND	2.41	IC REG BUCK ADJUSTABLE 3A 8SOIC	2	2	2	4.82	https://www.digikey.ca/en/products/detail/texa
									0	
Elec Toal									325.495	

Figure Appendix D-2. Elec BOM